Available online at www.CivileJournal.org

Civil Engineering Journal

(E-ISSN: 2476-3055; ISSN: 2676-6957)

Vol. 11, No. 04, April, 2025

Development of Oscillating Water Column Breakwater Model

Sugianto [1*], Rita Tahir Lopa [1], Riswal Karamma [1*], Chairul Paotonan [2]

[1] *Department of Civil Engineering, Hasanuddin University, South Sulawesi 91711, Indonesia.*

[2] *Department of Ocean Engineering, Hasanuddin University, South Sulawesi 91711, Indonesia.*

Received 23 December 2024; Revised 15 March 2025; Accepted 22 March 2025; Published 01 April 2025

Abstract

Integrating coastal protection functions and wave energy conversion makes the OWC breakwater an environmentally friendly and material-efficient innovation compared to conventional breakwaters. This research aims to determine the wave runup height on the Sloped side of the OWC breakwater model and its internal pressure. Utilizing theoretical approaches, a 1:20 scale laboratory model, dimensional analysis, and parameter relationships, the study investigates the effects of wave interaction, model geometry, and water depth. The analysis reveals a positive correlation between the combined parameter value (ψ) and relative pressure $(P/\rho g h_s)$, highlighting the consistent influence of these parameters on pressure behavior. Results show that a lower slope angle increases pressure, while variations in inlet opening sizes (h_s) significantly affect wave runup (R_u/H_i) and run-down (R_d/H_i). Larger inlet openings generally reduce the wave runup effect, though the magnitude of this impact depends on the slope angle. The optimal configuration for the OWC breakwater model is identified as an inlet opening size between 5 cm with a slope angle of 45° to 60°, providing relatively higher pressure while maintaining stability. This combination improves the system's efficiency in absorbing and using wave energy.

Keywords: Reflection; Runup; Pressure; Breakwater; Oscillating Water Column.

1. Introduction

An Oscillating Water Column (OWC) breakwater harnesses wave energy while protecting the coast. This model can be used on outer islands to reduce coastal erosion and generate electrical energy from wave motion. An Oscillating Water Column (OWC) breakwater offers dual benefits: offering renewable energy to outer islands and protecting coastal areas from the detrimental effects of ocean waves. Among wave energy concepts, the OWC system is considered one of the most extensively studied and advanced technologies [1]. By harnessing power from ocean waves, OWC breakwaters can serve as an energy source for outer islands. This system utilizes pressure fluctuations from waves entering the water column. The energy extracted can be converted into electricity utilized for island-specific needs. Nonetheless, site-specific evaluations of wave energy potential are crucial to assess the efficiency and reliability of these systems, especially given the varying wave characteristics across different outer islands.

Conventional rubble mound breakwaters require a significant amount of construction material and are associated with high costs. In deeper waters, the size of these structures must be increased, leading to further material demands and higher costs [2-4]. Additionally, rubble mound breakwaters rely on a strong subgrade foundation to withstand the forces acting upon them [3, 5]. The design and construction of resilient breakwaters depend on a thorough analysis of various factors, such as structural stability against wave forces, the calculation of wave propagation, and the interaction of breaking waves [6]. There are many alternative breakwaters with asymmetrical or sinking models that can be applied to

* Corresponding author: riswalchiwal@gmail.com; sugianto20d@student.unhas.ac.id

http://dx.doi.org/10.28991/CEJ-2025-011-04-02

reducing wave impact through wave deformation mechanisms [7]. Considering the natural resource constraints required for large-scale construction materials, economic considerations play a critical role in breakwater innovation. One such innovation is the development of hollow breakwaters, which offer a more sustainable solution. These columned structures are environmentally friendly, conserve structural materials, and serve a dual purpose as wave energy converters. By utilizing oscillating water column (OWC) technology, the water's motion inside the breakwater column generates air pressure through an opening at the top, enabling wave energy capture.

Studies examining the geometry of inlet openings and tilt angles in OWC system design have produced various findings. For instance, Iturrioz et al. [8] investigated small aperture sizes ranging from 2 mm to 50 mm using Open FOAM simulations, focusing on how wave height and Slot size affect system performance. Daniel Raj et al. [9] introduced the concept of a harbor wall to improve the hydrodynamic efficiency of OWC systems, but the geometry of the inlet opening was not explicitly analyzed. Research by Elhanafi et al. [10] explored the effects of underwater lip depth and thickness on OWC performance, emphasizing underwater geometric design rather than inlet openings. Similarly, Ning et al. [11] focused on U-shaped geometry by modifying the vertical channel height and available space width but does not explicitly address the variation in the inlet opening. Other studies, such as Vyzikas et al. [12] examined four distinct OWC geometries on chamber design. At the same time, Deng et al. [13] analyzed the ratio of openings at the top of the chamber relative to a horizontal bottom plate. Conversely, Mahnamfar & Altunkaynak [14] and Bouali & Larbi [15] explored the general optimization of OWC chamber geometry and various configurations to improve energy conversion without concentrating on specific inlet openings. Lastly, Oh & Han [16] directly investigated the impact of inlet geometry on wave energy capture efficiency, providing insights into how inlet design affects overall performance. These studies underscore extensive research on OWC geometries but have limited focus on the combined effects of inlet opening size and slope angle on hydrodynamic performance, a gap that this study seeks to address.

The principle of the OWC breakwater is a watertight structure with a column inside and an orifice at the top. Since the breakwater is shaped like a trapezoidal prism, it is important to study the wave deformation, wave runup, and pressure at the orifice. To determine the crest elevation of the breakwater structure based on the runup height, the runup height (R_u) and pressure (P) are influenced by the magnitude of the incident wave height (H_i), the inlet opening (h_s), and the slope angle (α).

The integration of OWCs with breakwaters is an innovative approach that offers a dual solution for renewable energy management and coastal protection. The research conducted shows the great potential of this approach, although there are still challenges that need to be overcome for large-scale implementation. With the development of technology and improved understanding of wave interaction with integrated structures, the development of OWC breakwaters becomes more feasible. Taking into account the efficiency of the structure by considering wave deformation, wave runup, energy capture, and the ease of applying empirical equations in structural planning is important in practice. The main objective of this research is to obtain the maximum wave runup on the OWC breakwater structure to determine the efficiency of the OWC breakwater shape and the performance of the oblique side OWC breakwater as a wave energy converter. The goal is to find the empirical equation that relates wave parameters, breakwater structure parameters, wave runup, and water column oscillation pressure.

This article is prepared to provide a systematic understanding of the research conducted. Section 1 presents the background of the research, explaining the issues and why the research is necessary, the importance of the research topic, its contribution to understanding or solutions to the problem, an overview, and the limitations of the issues to be studied.

- Conventional wave breakers, like rubble mounds, are inefficient for deep waters or remote areas due to their high material requirements, costs, and need for strong foundation support. Many studies on Oscillating Water Columns (OWC) have not emphasized the specific geometric effects, such as inlet opening size (h_s) and slope angle (α), on relative pressure efficiency and structural performance. Outermost islands require efficient solutions to reduce coastal erosion while simultaneously generating renewable energy, but the implementation of OWC in these areas faces challenges due to significant sea wave variability. Research is needed to evaluate how variations in geometric design (inlet opening and slope) can enhance relative pressure efficiency and wave runup on OWC breakwaters, which has not been "extensively researched."
- The importance of this research topic offers a dual solution: protecting the coast from the impacts of erosion while simultaneously generating renewable energy for remote islands that are difficult to connect to conventional energy networks. Integrating the functions of coastal protection and wave energy conversion makes the OWC breakwater an environmentally friendly and material-efficient innovation compared to traditional breakwaters. By examining the effects of inlet size and slope angle on relative pressure and wave runup, this study fills a gap in the literature that has previously lacked focus on these parameters.
- The contribution of this research will yield empirical equations that describe the relationship between wave parameters (H_i), breakwater structure parameters (h_s), and (α), as well as wave responses such as runup and

oscillation pressure. These findings will guide the design of more efficient and practical OWC breakwaters, particularly for applications in areas with limited resources. This study could be a key reference for optimizing OWC geometry to improve hydrodynamic efficiency, facilitating wider application in diverse wave conditions.

- The research description focuses on the effects of inlet opening size *(h_s)* and slope angle *(α)* on relative pressure *($P/\rho gh_s$)* and wave runup height *(R_u)* on the OWC breakwater structure. The analysis is conducted at specific water depths (17.5 cm, 21 cm, and 24.5 cm) to understand the system's response to "changes in these parameters."
- The scope of this study does not include other technical aspects such as structural materials, resistance to corrosion, or economic aspects of system implementation. The variation in inlet opening sizes is limited to values relevant to the experimental design, and the analysis focuses on relative pressure and wave runup as performance indicators. The research is limited to laboratory settings, necessitating further validation for large-scale field applications.

Section 2 describes the research methodology, including the experimental design, measures used, and data analysis methods. Section 3 presents research findings on how inlet opening size *(h_s)* and slope angle *(α)* affect relative pressure and wave runup at different water depths. Furthermore, the discussion regarding the implications of the research findings, comparisons with previous studies, and the evaluation of OWC breakwater efficiency is present in Section 4. Finally, Section 5 provides the main conclusions of this research, including the developed empirical equations and recommendations for the future development of OWC breakwater design.

2. Theoretical Foundation

2.1. Wave Deformation

As waves travel from the deep sea to shallow waters protected by coastal structures, their speed, height, and possibly direction change. However, the wave period is considered constant throughout its journey. The factors that cause this change in wave characteristics are the depth and depth variation of shallow water. Wave parameters change due to shoaling, refraction, and breaking. If a wave encounters an obstacle along its way, it will experience scattering (diffraction) [17].

Wave deformation events can be explained as follows: Wave refraction is a phenomenon in which the direction of motion of the wave crest changes or deflects; wave diffraction occurs when energy moves along the wave crest to a sheltered area; and wave reflection is the process of reflecting wave energy, usually caused by the presence of structures in the coastal area. Equation 1 describes the coefficient of wave reflection.

$$K_r = \frac{H_r}{H_i} = \sqrt{\frac{E_r}{E_i}} \tag{1}$$

Here, K_r represents the refraction coefficient, H_r denotes the height of the reflected wave, H_i refers to the height of the incident wave, E_r indicates the energy of the reflected wave, and E_i signifies the energy of the incident wave. The building reflection coefficient is estimated based on model tests, where the reflection energy is E_r = ½$\rho gHr2$ and the incident wave energy is E_i = ½$\rho gHi2$, where ρ is the mass density of the liquid and g is the acceleration of gravity. The value of K_r ranges from 1.0 for total reflection to 0 for no reflection. The values of K_r in energy-absorbing building types are shown in Table 1 [17].

Table 1. Reflection Coefficient

Energy-absorbing building type	K_r
Vertical wall with a peak above the water	0.7 – 1.0
Vertical wall with submerged top	0.5 – 0.7
Sloping side stone pile	0.3 – 0.5
Concrete block piles	0.3 – 0.5
Vertical building with energy absorbers (with holes)	0.05 – 0.2

2.2. Wave Energy

Wave energy can be categorized into two types: kinetic energy, generated by the movement of particles due to wave motion, and potential energy, caused by the displacement of the water surface as waves pass. According to the theory of small-amplitude waves, when wave energy is measured relative to the still water level and all waves propagate in the same direction, the kinetic and potential energy components are equal [17]. The total energy per unit width of a wave over one wavelength is described by Equation 2.

$$E_t = E_k + E_p = \frac{\rho g H^2 L}{8} \tag{2}$$

The mean energy per unit area is represented in Equation 3.

$$E = \frac{E_t}{L} = \frac{\rho g H^2}{8} \tag{3}$$

where E_k is the kinetic energy unit wavelength width (joule/m), E_p is the potential energy unit wavelength width (joule/m), E_t is the total energy unit wavelength width (joule/m), E is the average wave energy unit area (joule/m^2), H is the wave height (m), ρ is the mass density of water (kg/m^3), g is the acceleration of gravity (m/s^2). Wave power *(P)* is the wave energy per unit time in the direction of wave propagation.

$$P = \frac{nE}{T} \tag{4}$$

where, n is the wave energy factor valued in Equation 5.

$$n = \frac{1}{2}\left(1 + \frac{2kd}{\sin h2kd}\right) \tag{5}$$

2.3. Wave Runup

When a wave hits a building, it will rise (run-up) on the building surface, shown in Equation 6 [17]. Where *Ir* is the Iribarren number, θ is the angle of inclination of the breakwater side (°), *H* is the wave height at the building site (m), L_o is the wavelength (m). Runup is used to determine the elevation of the beach building lighthouse, while rundown is used to calculate the stability of rip-rap or revetment.

$$Ir = \frac{tg\theta}{\left(\frac{H}{L_o}\right)^{0.5}} \tag{6}$$

2.4. Water Column Oscillating

To determine the wave forces there are several theories that can be used, but in this experiment using airy theory or simple wave theory [18]. To calculate the pressure going to the orifice using Equation 7.

$$P_2 - P_0 = \rho\left(\frac{A_1}{A_2}\right)\frac{\partial\varphi_1}{\partial t} + \rho\frac{Q}{A_1}(v_2 - v_1) \tag{7}$$

where P_2 represents the air pressure at the orifice (Pa), P_0 is the atmospheric pressure outside the system (Pa), g is the gravitational acceleration (m/s^2), T denotes the wave period (sec), f_c is the resonant frequency of oscillation in the column area (Hz), ω_c is the angular frequency of the wave in the column area (rad/s), v_1 indicates the velocity of air flowing within the OWC column (m/s), v_2 refers to the velocity of air passing through the orifice (m/s), A_1 represents the cross-sectional area of the OWC column (m^2), A_2 denotes the cross-sectional area of the orifice (m^2), Q_1 is the air flow rate in the OWC column (m^3/s), Q_2 is the air flow rate at the orifice (m^3/sec), φ_1 corresponds to the potential velocity in the OWC column (rad.m/s), and φ_2 is the potential velocity at the orifice (rad.m/s).

2.5. Model Basic Law

The basic concept of modeling using scale models is to replicate a real-world problem or phenomenon on a smaller scale, ensuring that the behavior observed in the model matches that in the prototype. This basic concept is achieved through geometric, kinematic, and dynamic fit [19]. The Relationship between the model and the prototype is defined by scaling because scaling governs how the physical characteristics of the model compare to the original prototype, with each parameter having a unique scale factor. Scale refers to the ratio of a parameter's value in the prototype to its corresponding value in the model.

Geometric congruence refers to a condition where the model maintains the same shape as the prototype, though its size may differ. The ratio of all corresponding lengths between the model and the prototype remains constant. There are two types of geometric congruence: perfect geometric congruence (without distortion) and geometric congruence with distortion (distorted). In a geometrically ideal model, the length scale in the horizontal direction and the length scale in the vertical direction are the same, while in a distorted geometric model, the length scale and height scale are not the same. If possible, the model should be scaled without distortion so that the results of tests or simulations performed on the model remain valid and can represent the actual conditions of the prototype. However, in some cases, distorted models are used when technical or practical limitations prevent the creation of a genuinely proportional model, for example, due to space or cost constraints in making physical models. Geometric equivalence can be expressed in the form of Equations 8 and 9 as follows:

$$n_L = \frac{L_p}{L_m} \quad (8)$$

$$n_h = \frac{h_p}{h_m} \quad (9)$$

with n_L being the length scale, n_h being the height scale, L_p being the length of the prototype, L_m being the length of the model, h_p being the height of the prototype, and h_m being the height of the model.

Kinematic congruence is a congruence that satisfies the criteria of geometric congruence, and the comparison of velocity and acceleration of the flow at two points on the model and prototype in the same direction is the same. In the model without distortion, the ratio of velocity and acceleration in all directions is the same. For the application of models with distortions, the scale ratio is usually not uniform in all directions, usually applied in the vertical or horizontal direction due to space, cost, and technical aspects such as sensor resolution or material thickness. The velocity scale n_v, the discharge scale notated n_Q, time scale n_t are defined in Equations 10 to 12.

$$n_V = \frac{V_p}{V_m} = \frac{\left(\frac{L_p}{t_p}\right)}{\left(\frac{L_m}{t_m}\right)} = \frac{L_p t_m}{L_m t_p} = \frac{n_L}{n_t} \quad (10)$$

$$n_a = \frac{a_p}{a_m} = \frac{\left(\frac{V_p}{t_p}\right)}{\left(\frac{V_m}{t_m}\right)} = \frac{V_p t_m}{V_m t_p} = \frac{n_L}{n_t n_t} = \frac{n_L}{n_t{}^2} \quad (11)$$

$$n_t = \frac{t_p}{t_m} \quad (12)$$

Dynamic congruence fulfills the criteria of geometric and kinematic congruence, and the ratio of forces acting on the model and prototype for all flows in the same direction is equal. The forces are inertial force, pressure force, weight force, friction force, springy force, and surface tension. Some dynamic constructs are the Reynold number, which describes the ratio of inertial force to friction force; the Froude number; the Froude number, which is the ratio of inertial force and gravitational force; the Cauchy number, which is the ratio of inertial force and elastic force; and the Weiber number, which is the ratio between inertial force and surface tension force.

2.6. Dimensional Analysis Method

Dimensionless numbers are used to express relationships between parameters and are used to describe research results. Determining the dimensionless number can be done by dimensional analysis [19]. Buckingham Pi theory is the relationship between a function expressed in terms of dimensional parameters and another function expressed in terms of nondimensional parameters. Buckingham PI theory aims to obtain a nondimensional number or numbers. A physical problem has '*n*' parameters, one of which is an independent parameter, then the relationship between these parameters is expressed:

$$q_1 = f(q_2, q_3, \ldots q_n) \quad (13)$$

where $q1$ is the independent variable, q_2, q_3,...q_n are n-1 independent variables. Equivalent mathematical statements:

$$g(q_1, q_2, q_3, \ldots q_n) = 0 \quad (14)$$

where g is any function that is not f.

Buckingham PI theory states that in a physical problem with n quantities where there are m dimensions (except in some cases), there will be n-m dimensionless parameters or called π parameters, which satisfy the equation:

$$G(\pi_1, \pi_2, \pi_3 \ldots \pi_n) = 0 \quad (15)$$

$$\pi = G_1(\pi_2, \pi_3, \ldots \pi_{n-m}) \quad (16)$$

The relationship between the parameters (dimensionless numbers) is determined experimentally, not using the Buckingham PI theory. The procedure for determining the non-dimensional group (π) as follows:

1. Arrange all the variables involved, write the primary dimensions of the variables above, and write all the dimensions of the variables according to the primary dimensions used.
2. Select the "repeated variable" with the number equal to r, and all primary dimensions are in the repeated variable.
3. Recurring variables are variables that are used in the calculation of all π groups. Recurring variables can appear in π, so do not mistakenly select an independent variable as a recurring variable.

4. Set up *(n-m)* equations to get dimensionless groups.

5. Determine π groups if the variables can be expressed in different dimensional systems.

3. Research Methodology

3.1. Research Location and Variables

The study was carried out in the Hydraulics Laboratory of the Civil Engineering Department, Faculty of Engineering, Hasanuddin University, located in Gowa, South Sulawesi. The variables studied were wave runup (R_u), pressure (P), wave period (T), wave height (H_i), water depth (d), inlet opening (h_s) and slope angle (α). The breakwater model in this study, the model made is based on the concept of coastal protection which also captures wave energy. The OWC wave flume model is shaped like a trapezoidal prism and has an inlet hole with a side opening water column and has a hole on top to release air pressure from inside the model space. Figure 1 is the side view of the wave flume, and the position of the model and Figure 2 is the plan of the OWC wave combustor model.

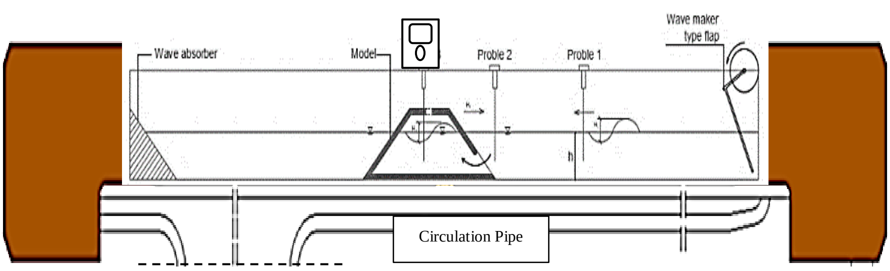

Figure 1. Side view of the wave flume and model position

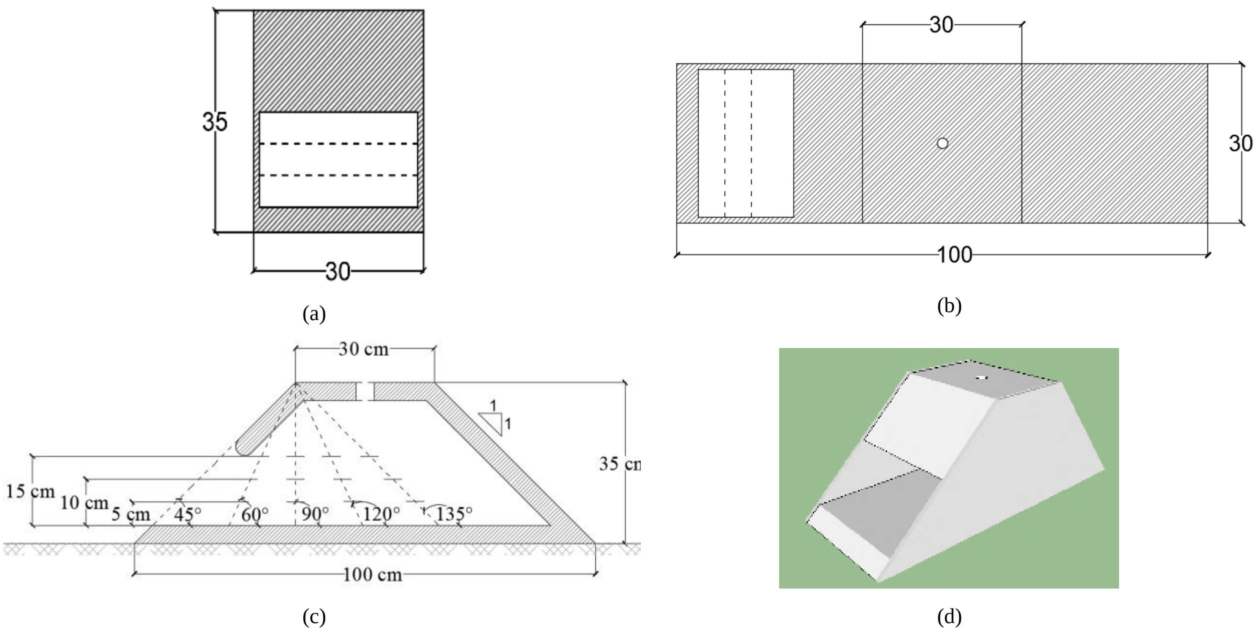

Figure 2. (a) OCW breakwater model with front view, (b) top view, (c) side view of the model with slope and opening variations, and (d) model perspective

The wave flume is constructed with a steel frame and glass walls and is equipped with a wave generator and a wave damping device. The channel has dimensions of 15 m in length, 0.3 m in width, and 0.5 m in height, with an effective water depth of 0.46 m. It is also integrated with a computer system running wave measurement software, which records and outputs wave height readings, including H_{max} and H_{min}. The model tests were conducted at a scale of 1:20 based on the principle of hydrodynamic similarity (Froude similarity), which ensures that dominant forces such as gravity are accounted for in the hydrodynamic similarity principle, and this scale is commonly used in laboratory modelling of coastal infrastructure. Figure 3 shows the wave generator used in the laboratory for research.

Figure 3. Model of wave flume and flap type wave generating machine

The wave-generating machine used in this study is a flap type. Waves are generated by a flap-type wave generator, in which the lower part of the flap is equipped with a hinge, while the upper part of the flap is connected to the drive disc through a stroke system. The flap movement is a rotational movement controlled through the rotation of the drive disc. It is this reciprocating movement of the flap that serves to generate waves.

Devices used for wave reading include wave probes, wave monitors, and computers. The wave probe plays a role in measuring the water level or wave elevation, which is then reported through the wave monitor and recorded using the WVFW (Wave View for Windows) application. The characteristics of waves commonly generated by wave generators in wave generation channels range from 2 to 12 cm, with periods ranging from 0.6 to 6 seconds. The type of wave generated is a regular wave. The wave height can be varied through adjustments to the stroke or disc in a wide range of variations, aiming to change the amount of flap deviation. Similarly, the wave period *(T)* can be adjusted by adjusting the rotational speed of the disc. A wave damper or wave absorber is used to dampen the waves at the end of the wave channel. In this study, the wave damper is a pile of rubber with coarse fibres like a mat placed under the water surface layer.

3.2. Research Tools and Materials

In carrying out the OWC breakwater physical modelling process, the tools and materials used in the laboratory research consist of:

- Wave flume equipped with wave drive and wave height reading unit.
- Millimetre paper for measuring runup and rundown wave height.
- Pressure gauge for measuring air pressure.
- Camera for documentation.
- Recording form and stationery.
- Mechanical equipment to replace pulley and stroke.
- Workshop equipment for making models.
- The model materials used in the research are acrylic for model making and additional materials for adhesives and screws.

3.3. Model Scale and Simulation Design

The model scale is determined based on the variables under investigation, while the design of the OWC breakwater model considers the laboratory facilities, available materials, and measurement precision. The scale and dimensions of the model are detailed in Table 2.

Table 2. Model dimensions

Dimensions	Prototype (m)	Model (cm)
High	7	35
Top length	6	30
Bottom length	20	100
Inlet slope (h_s)	1, 2, 3	5, 10, 15
Slope (θ = 1,2,3,4,5)	45°, 60°, 90°, 120°, 135°	45°, 60°, 90°, 120°, 135°

This study was conducted based on experimental variations designed for each parameter. There were 55 test variations for each slope *(α)* model of the OWC breakwater, with simulation variations including opening variation *(h_s)*, depth variation *(d)*, and wave period *(T)*. Table 3 presents the model simulation scenarios, and the parameters used in the study.

Table 3. Simulation scenarios and research variations

Slope model *(α)* (°)	Inlet opening *(hs)* (cm)	Water depth *(d)* (cm)	Period *(T)* (sec)
Slope 45	5, 10, 15	17.5, 21, 24.5	1.1, 1.2, 1.3, 1.4, 1.5
Slope 60	5, 10, 15	17.5, 21, 24.5	1.1, 1.2, 1.3, 1.4, 1.5
Slope 90	5, 10, 15	17.5, 21, 24.5	1.1, 1.2, 1.3, 1.4, 1.5
Slope 120	5, 10, 15	17.5, 21, 24.5	1.1, 1.2, 1.3, 1.4, 1.5
Slope 135	5, 10, 15	17.5, 21, 24.5	1.1, 1.2, 1.3, 1.4, 1.5

3.4. Research Implementation

The simulation was carried out by first taking measurement data of water depth *(d)* against the model height *(B)* with variations of 0.5, 0.6, and 0.7 against the model height. Data collection and observation of wave height were measured and recorded at 2 points in front of the model. The implementation of wave height measurement, runup, rundown, reflection, and pressure measurement are carried out when the generated waves are in a stable condition after being produced. The implementation procedure is as follows:

- The wave breaker structure used as a research model is placed in the center of the wave flume, as shown in Figure 1.
- Fill the wave flume with water based on the predetermined variations in water depth.
- Set the wave period by rotating the variation on the main machine, then adjust the flap displacement according to the stroke scale.
- Adjust the position of the probes. For probes 1 and 2, they are set in front of the model at positions ½ and ¼ of the wavelength, according to the depth and wave period.
- Calibrate the probes to facilitate data recording on the WVFW software, with readings from probes 1 and 2 starting from point 0 (water surface).
- Setting the duration of data collection by adjusting the frequency on the WVFW and determining the number of wave samples.
- Initiate the collection of wave height data, wave reflection, runup, rundown, and pressure by pressing the 'wave maker start' button on the control panel, then commence data recording by the WVFW when the waves are stable or shortly after the waves are generated.
- Stop data recording after the wave graph appears on the monitor, then turn off the machine by pressing the 'wave maker stop' button on the control panel.
- Convert the WVFW reading data into '.xlsx' format by using the export command on WVFW.
- Performing steps 1-9 for each parameter variation.

3.5. Research Visualization Sketch

The visualization sketch of runup (the maximum height of waves rising to the surface of the breakwater) and rundown (the maximum height of waves descending after runup) on the OWC breakwater model can be seen in Figure 4 to understand the wave interaction patterns with variations in slope, inlet size *(h_s)*, and water depth *(d)*.

Figure 4 illustrates four variations of the inlet opening parameter *(h_s)*, slope *(α)*, and water depth *(d)* as a visualization sketch of the research. The inlet channel opening affects the efficiency of wave energy capture, while the slope influences the stability of the structure and hydrodynamic performance. The research sketch describes the visualization components where the x-axis shows the slope of the wave breaker (45°, 60°, 90°, 120°, 135°). The y-axis shows the conditions of high runup, and rundown (m) measured from the average water surface. The water depth measurements *(d)* include 17.5 cm, 21 cm, and 24.5 cm. The Inlet size *(h_s)* includes closed conditions, 5 cm, 10 cm, and 15 cm. The points to be analyzed are the effects of slope variations, how slopes of 45° to 135° influence the runup and rundown patterns, and the visualization of wave energy flow on gentle versus steep slopes. The inlet sizes (hs), the comparison of closed inlets at 5 cm, 10 cm, and 15 cm on OWC efficiency, and the relationship between inlet size and water oscillation amplitude within the chamber. The influence of water depth *(d)*, the effect of three water depths on relative pressure *($P/\rho g h_s$)* and water oscillation, and the impact of depth on the effectiveness of the OWC model in dissipating wave energy. The combination of effects (slope-inlet-depth) and how the combination of slope, inlet, and depth creates synergistic effects or trade-offs.

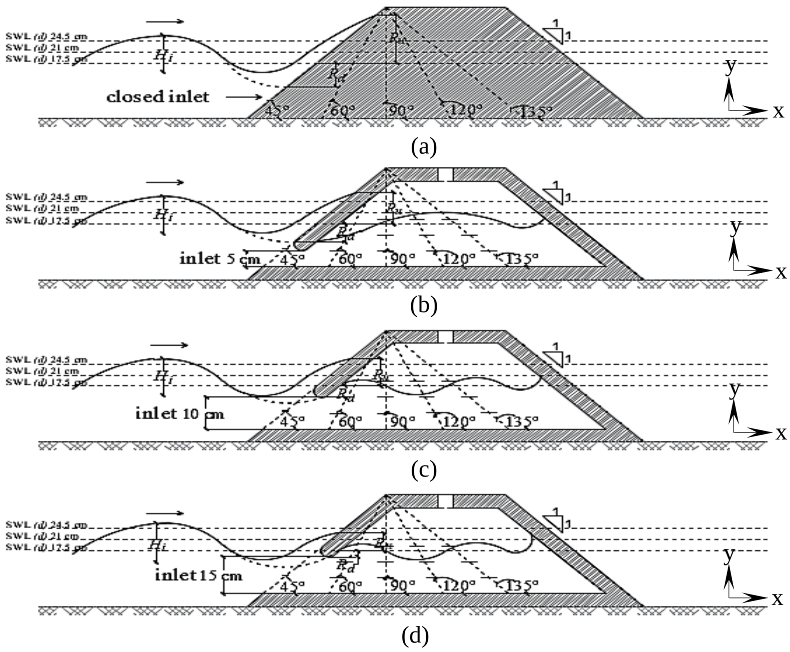

Figure 4. Visualization sketch of wave runup and rundown (inlet closed (a), 5 cm (b), 10 cm (c), and 15 cm, as well as variations in slope and flow depth)

The flowchart of the research process is a visual representation of the steps or stages taken in the research. It helps to provide a clear overview of the research flow, from the initial stage to the final stage. The research flowchart is shown in Figure 5.

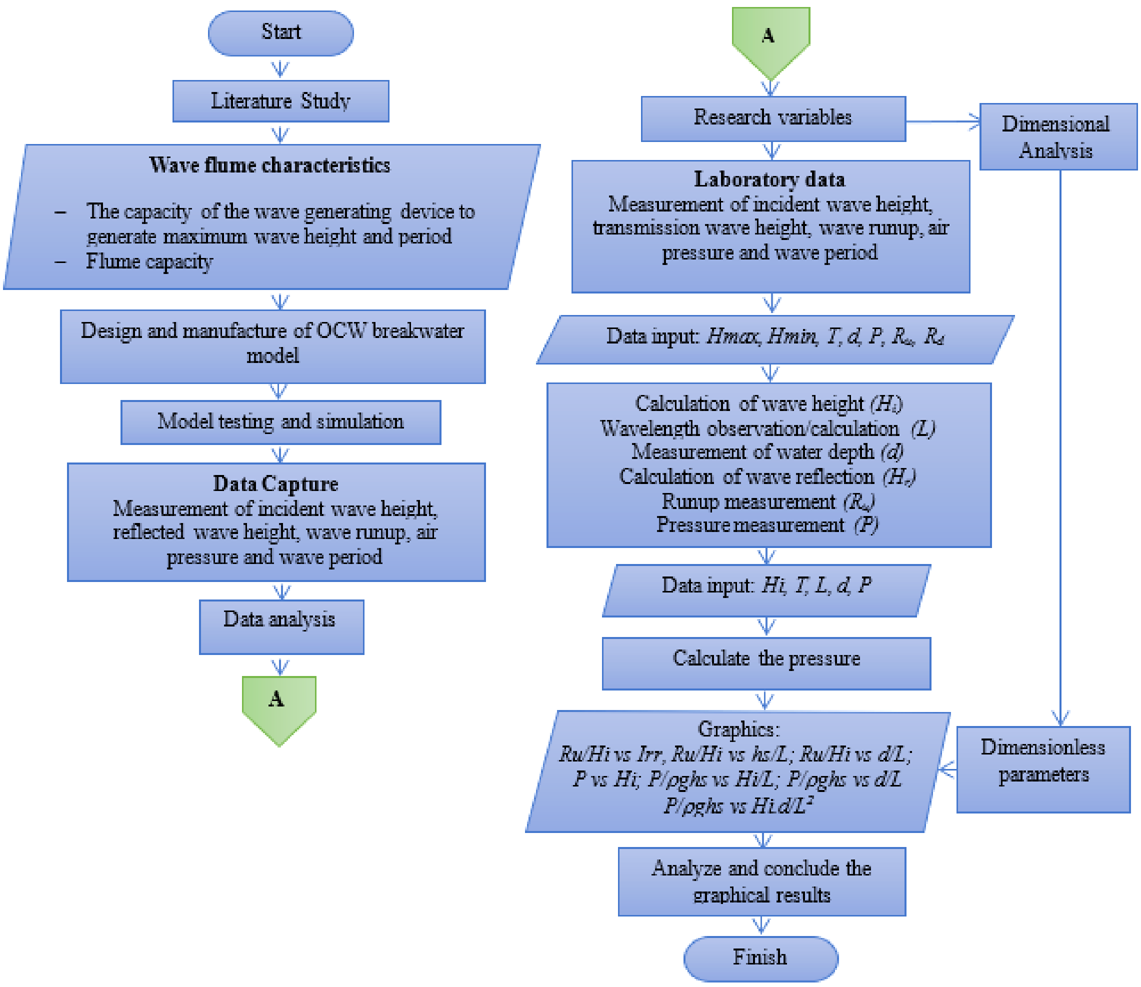

Figure 5. Research flow diagram

The initial stage is the literature study, which involves conducting a literature review related to previous research concerning OWC breakwaters and understanding the capacity of wave generation devices in producing wave height and maximum wave period. It is essential to know the capacity of the flume that will be used in the testing. Wave Flume Characteristics involve determining the characteristics of the flume, including capacity and wave measurement parameters.

The main processes carried out are the design of the OWC wave breaker model and the creation of the OWC wave breaker model, namely designing and creating a wave breaker model based on OWC. Model testing and stimulation, namely conducting testing and simulation of the breakwater model in the laboratory. Data capture, namely by measuring wave parameters such as incident wave height, reflected wave height, wave runup, air pressure, and wave period.

Data analysis is processing and analyzing data to gain an understanding of the model's behavior. Determination of research variables is determining the variables to be used in the study, such as wave height, wave transmission, air pressure, and runup. The laboratory stage is collecting laboratory data by measuring parameters such as incoming wave height, wave transmission height, wave runup, air pressure, and wave period.

Data input is entering data such as H_{max}, H_{min}, T, d, P, R_u, R_d. Calculation and analysis are calculating wave height (H_i), observation or calculation of wavelength (L), water depth (d), reflection coefficient (H_r), runup (R_u), and pressure (P). Dimensional analysis is conducting dimensional analysis to identify dimensionless parameters such as the relationship between R_u/H_i and Ir, the relationship between R_u/H_i and h_s/L, the relationship between R_u/H_i and d/L, the relationship between P and H_i, the relationship between $P/\rho gh_s$ and Hi/L, the relationship between $P/\rho gh_s$ and d/L, and the relationship between $P/\rho gh_s$ and $H_i.d/L^2$.

The final section interprets and provides conclusions from the results of analyzing the graph results to conclude the behavior of the OWC model based on the parameters tested and then provides recommendations for OWC design and performance. The research method above has explained using a flume wave generator to create waves with measurable characteristics. The experimental process involves parameters measured with accurate instruments, such as wave height, runup, air pressure, and wave period.

4. Results and Discussion

4.1. Wave Height

Wave height data validation in tests without a breakwater ensures the reliability of the obtained data. This process also verifies the accuracy of measuring instruments in capturing wave height, enabling further analysis. Validation is performed by comparing the results with previous studies [20, 21], focusing on wave period (T) and wave height (Hi). The results of the wave height study were juxtaposed with the results of Dean and Dalrymple's calculations regarding hydrodynamic characteristics for porous sea walls protected by submerged breakwaters. The wave height data in this study follows a similar trend and aligns with the findings of Huddiankuwera et al. [21] and Dean & Dalrymple [22], as shown in Figure 6.

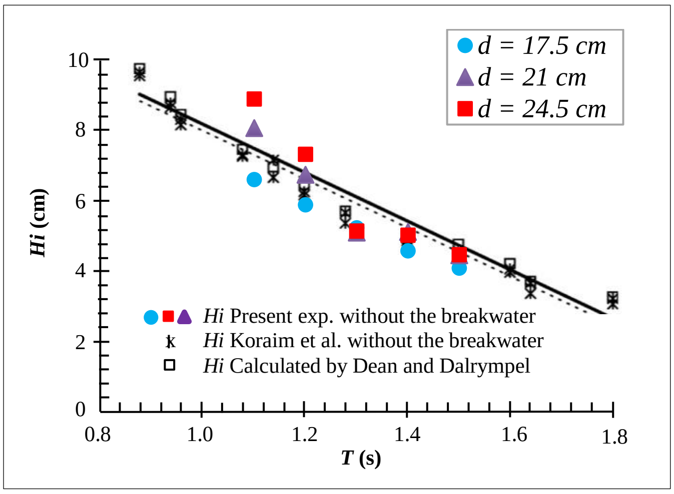

Figure 6. Wave height data validation

4.2. Water Level Fluctuation

Data on water level fluctuations were obtained by converting the time series recorded by the wave probe, with the calibration results of the wave probe adjusted based on the variation in water depth for each specific probe. With 250 samples recorded, the water level fluctuations at wave probes 1 and 2 are depicted in Figures 7 to 9. The experiments were recorded using variations in water depth (d) of 17.5 cm, 21 cm, and 24.5 cm, and wave periods (T) of 1.1, 1.2, 1.3, 1.4, and 1.5 seconds, as designed variations for each model.

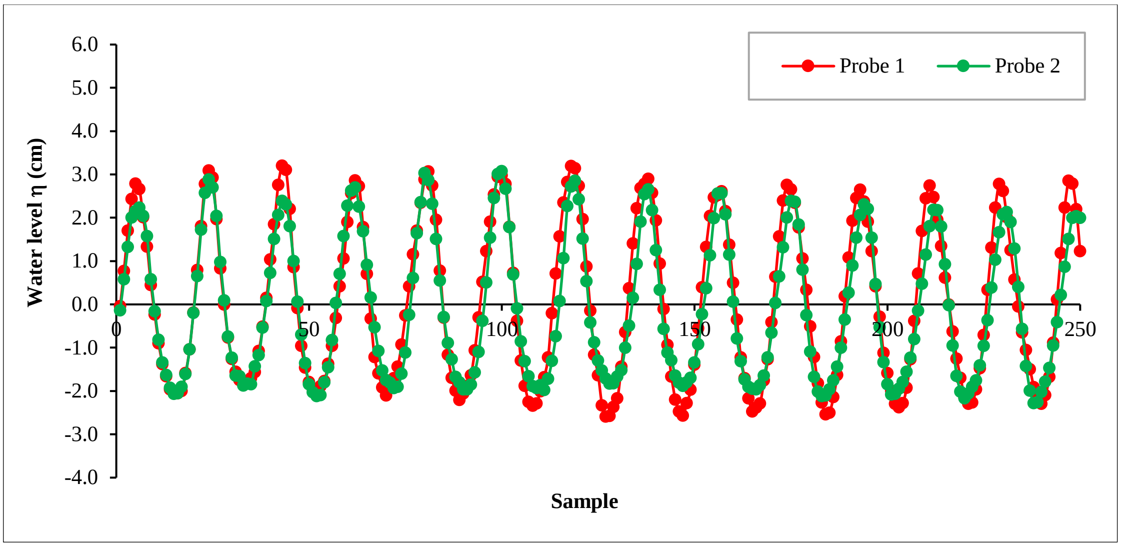

Figure 7. Change in water surface height at depth *(d)* 17.5 cm

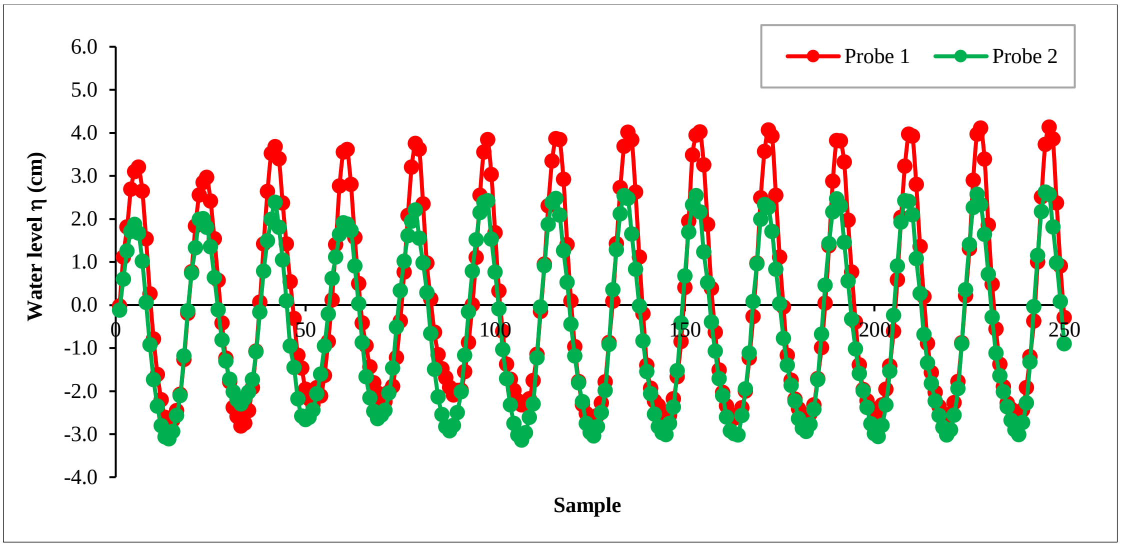

Figure 8. Change in water surface height at depth *(d)* 21 cm

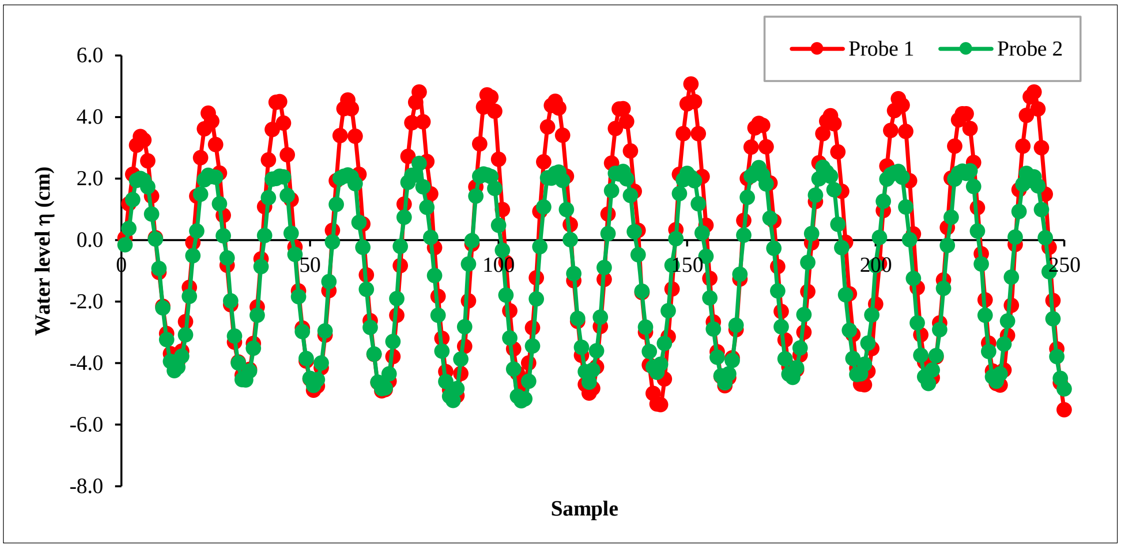

Figure 9. Change in water surface height at depth *(d)* 24.5 cm

Figures 7 to 9 demonstrate that the waves are sinusoidal graphs, allowing the maximum and minimum wave heights to be determined. Table 4 presents the complete data on wave characteristics resulting from the study's variations.

Table 4. Wave characteristics at *(d)* 17.5 cm, 21 cm, and 24.5 cm and the ratio of *d* to *H/L* change

d (cm)	*T* (s)	H_{max}	H_{min}	*H* (cm)	*L* (cm)	*H/L*
17.5	1.1	4.676	4.211	6.782	147	0.046
	1.2	3.531	3.474	5.268	165	0.032
	1.3	4.107	3.760	5.987	182	0.033
	1.4	3.063	2.964	4.544	198	0.023
	1.5	2.754	2.628	4.068	215	0.019
21	1.1	5.953	4.877	8.391	139	0.060
	1.2	3.540	3.346	5.213	153	0.034
	1.3	4.843	4.169	6.928	171	0.041
	1.4	3.453	3.378	5.142	186	0.028
	1.5	3.072	2.670	4.407	201	0.022
24.5	1.1	6.654	5.308	9.308	130	0.072
	1.2	3.461	3.408	5.165	144	0.036
	1.3	5.246	4.659	7.576	158	0.048
	1.4	3.453	3.314	5.110	172	0.030
	1.5	3.308	2.772	4.693	186	0.025

From the measurement data of 250 samples from probes 1 and 2, the regression formula yields the H_{max} and H_{min} values for each probe. The simulation results of wave height data collection obtained from automatic recording from a computer equipped with wave monitoring software and Eagle DAQ if converted into the calculation of wave steepness *(H_i/L)* with wavelength according to water depth, the comparison results show significant differences between *(d)* 17.5 cm, 21 cm, and 24.5 cm. One of the wave interval calculation results in period 1.1 with stroke 6 has a wave height interval H_{max} of 5,549 cm and H_{min} of 4,942 cm at a depth of *(d)* 17.5 cm, at a depth of *(d)* 21 cm has a wave height interval H_{max} of 7,028 cm and H_{min} of 5,841 cm, and at a depth of 24.5 cm has a wave height interval H_{max} of 8,337 cm and H_{min} of 6,130 cm.

4.3. Pressure Measurement

Pressure data validation in the experiment is conducted to confirm the reliability of the obtained results and to ensure the accuracy of the instruments used in measuring the pressure generated by the OWC breakwater, thus enabling further testing. The experimental measurement results are compared with theoretical results, and the percentage error and the value of (*R*) are determined. Figure 10 presents the results in graphical form, illustrating the relationship between wave height (H_i) and pressure (*P*) at depths of 17.5 cm, 21 cm, and 24.5 cm. The graphical results show the same trend, although there is an insignificant numerical difference.

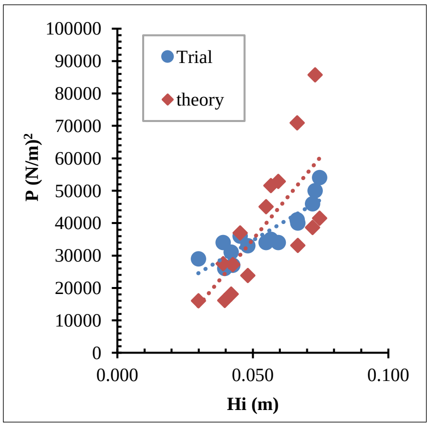

(a)

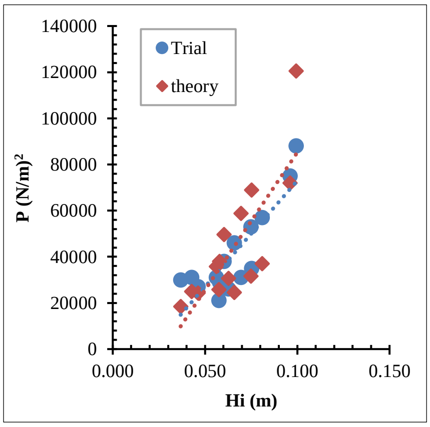

(b)

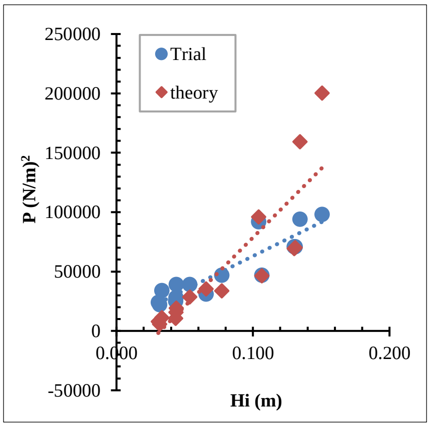

(c)

Figure 10. Experimental and theoretical pressure measurement results for water depths (*d*) of (a) 17.5 cm, (b) 21 cm, and (c) 24.5 cm

The *R*-value obtained from the experiment and theoretical calculations, based on the criteria for the *R*-value, indicates a strong to very strong correlation between the theoretical and experimental results. The *R*-value range observed is between 0.7986 and 0.9192. According to Soewarno [23], the correlation coefficient is a statistical measure of the covariance or relationship between two variables. To interpret the strength of this relationship, the following criteria are used: $R = 0$ (no correlation), $0 < R \leq 0.25$ (very weak correlation), $0.25 < R \leq 0.50$ (moderate correlation), $0.50 < R \leq 0.75$ (strong correlation), $0.75 < R \leq 0.99$ (very strong correlation), and $R = 1.00$ (perfect correlation). The error rate deviation, based on the Mean Absolute Error (MSE), ranges from 0.2240 to 0.2693, indicating that the accuracy of both the experimental and theoretical results is very good, as evidenced by the relatively small error rate. In research on the mathematical modeling of oscillating water columns, which compares the pressure drop between experimental and theoretical results, the average value and waveform are nearly identical [24].

4.4. Dimensional Analysis

The dimensional analysis has important objectives as it aims to understand the relationships between variables, to form groupings of variables into dimensionless parameters (reducing the number of variables in the form of parameters), to maintain the consistency of relationships between variables, and to avoid spurious relationships, to assist in determining methods and the implementation of data collection (simulation and surveys), to aid in creating model scales, and to help find concise relationships between variables in the form of equations or formulas.

The dimensional analysis performed by the Pi Buckingham method obtained dimensionless parameters, for the relative runup height can be expressed as shown in Equation 19 below:

$$f\left(\frac{Ru}{Hi}, Ir, \frac{h_s}{L}, \frac{d}{L}\right) = 0 \tag{17}$$

$$\frac{Ru}{Hi} = f\left(Ir, \frac{h_s}{L}, \frac{d}{L}\right) \ or \ \frac{R_u}{H_i} = f\left(Ir.\frac{h_s \cdot d}{L^2}\right) \tag{18}$$

With the height of the run-up (Ru) stated as shown in Equation 15.

$$\frac{R_u}{H_i} = f\left(Ir.\frac{h_s \cdot d}{L^2}\right) \tag{19}$$

Factors that affect runup *(R_u)* are flow depth *(d)* where the depth of water around the structure affects how waves interact with the breakwater. Inlet opening *(h_s)* where the size of the inlet opening affects the amount of water that can enter the structure, which in turn affects runup *(R_u)* and rundown *(R_d)*. Wave period and height *(T, H_i)* where waves of a certain period and height will interact differently with the structure, affecting runup *(R_u)* and rundown *(R_d)*. Using dimensionless variables allows comparison and generalization of analysis results for various wave and structural conditions. For ease of writing, dimensionless numbers are $\left(Ir.\frac{h_s \cdot d}{L^2}\right)$ are denoted by (ζ).

Changes in air pressure in the OWC breakwater model can be expressed in a functional relationship as can be seen in Equation 22 as follows:

$$f\left(\frac{P}{\rho g Hi}, \frac{Hi}{L}, \frac{d}{L}\right) = 0 \tag{20}$$

$$\frac{P}{\rho g h_s} = f\left(\frac{Hi}{L}, \frac{d}{L}\right) \text{ or } \frac{P}{\rho g h_s} = f\left(\frac{H_i \cdot d}{L^2}\right) \tag{21}$$

The air pressure in the OWC breakwater model stated as shown in Equation 18.

$$\frac{P}{\rho g h_s} = f\left(\frac{H_i \cdot d}{L^2}\right) \tag{22}$$

The pressure change in the OWC breakwater model can be expressed in terms of a functional relationship $\frac{P}{\rho g h_s} = f\left(\frac{H_i \cdot d}{L^2}\right)$ this shows that the pressure is affected by the combination of several physical parameters in a certain form. The air pressure *(P)* refers to the pressure generated by the oscillation of water in the column. The wave height *(H_i)* is the maximum crest height of the water wave. The inlet opening height *(h_s)* represents the height of the opening through which water enters the column. Flow depth *(d)* is the depth of water within the OWC column. The wave period *(T)* is the time it takes for one complete wave cycle. Gravitational acceleration *(g)* is the constant of Earth's gravity. Water density *(ρ)* is the mass per unit volume of water. To simplify the expression of dimensionless parameters, the combination is represented by $\left(\frac{H_i \cdot d}{L^2}\right)$, denoted as ($\psi$). The dimensionless parameters $\psi = \left(\frac{H_i \cdot d}{L^2}\right)$ and $\zeta = \left(Ir.\frac{h_s \cdot d}{L^2}\right)$ standardize the results for broader applicability across various conditions.

In the context of research on the development of the Oscillating Water Column (OWC) model as a wave breaker, the effects of experimental scale play a crucial role in evaluating and understanding the relationship between various design parameters (such as slope, inlet size, and water depth) and response variables such as relative pressure *($P/\rho g h_s$)*, wave deformation, or the energy efficiency produced. The significance of the effects of experimental scale in the development of the OWC model is:

- Measuring the impact of design parameters, the effects of experimental scale can help explain how changes in design parameters (such as slope angle or inlet size) affect system responses such as relative pressure $(P/\rho g h_s)$. If variations in slope (α) result in significant changes in pressure, then the scale effect value will indicate the magnitude of this influence compared to other parameters.
- Assisting in the identification of dominant parameters by measuring the scale effect, it can determine which parameters (slope, inlet size, water depth, or resonance) contribute the most to the system response, thereby allowing for a focus on optimizing design for those parameters.
- Validating practical relevance in the design of OWC-based wave breakers, statistically significant effects may not be practically relevant. The scale effect helps ensure that design changes provide tangible benefits for operation in real-world environments.

In Oscillating Water Column (OWC) wave studies, scale effects can measure how slope variations influence relative pressure $(P/\rho g h_s)$. These values help determine whether small design changes, such as inlet size or tilt angle, significantly impact OWC system performance.

4.5. Effect of Non-Dimensional Parameters (ζ) on Runup and Rundown

To examine the influence of (ζ) with runup and rundown, a simulation of 45° and 60° slope models with closed (h_{tutup}) and open (h_s = 5 cm, 10 cm, and 15 cm) inlets at a water depth (d) of 17.5 cm was used. From the graph, the relative runup value (R_u/H_i) tends to be greater at a slope of 45° than at a slope of 60°. In Figure 11-a for 45° and 60° slope variations (α) at an open inlet (h_s) of 0.05 m, it can be seen that the larger value of the non-dimensional parameter (ζ) causes the trend of the relative runup to be larger for a 45° slope. In contrast, at a 60° slope, the larger value of the non-dimensional parameter (ζ) causes the relative runup trend to decrease. The relationship of (ζ) with R_u/H_i and R_d/H_i presented in Figure 11-b for 45° and 60° slope variations (α) at an open inlet (h_s) of 0.10 m shows consistency. That is, the value of the non-dimensional parameter (ζ) provides similar trends in R_u/H_i and R_d/H_i at inlet opening (h_s) 0.10 m for both slope inclinations. In Figure 11-c for 45° and 60° slope variations (α) at inlet opening (h_s) 0.15 m, it can be seen that as the value of the non-dimensional parameter (ζ) increases, the relative runup tends to decrease at 45° slope. In contrast, at a slope of 60°, the larger value of the non-dimensional parameter (ζ) causes the relative runup trend to flatten, not experiencing significant changes. The relative runup value is larger at a slope of 45° compared to 60°, indicating that the waves climb more easily to the breakwater with a gentler slope. The relationship of non-dimensional parameters (ζ) to relative runup varies with slope. At a slope of 45° increasing these non-dimensional parameters tends to increase the relative runup, while at a slope of 60°, increasing these parameters tends to decrease or stabilize the relative runup. Changing the inlet opening has a consistent effect on R_u/H_i and R_d/H_i, with larger inlet openings generally reducing runup and rundown effects, although this effect can vary based on the slope and the non-dimensional parameters used.

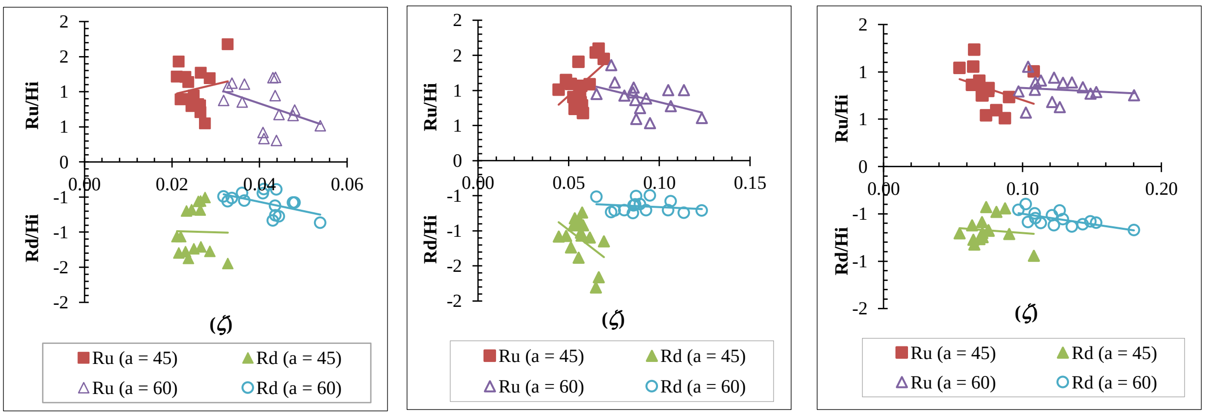

(a) (b) (c)

Figure 11. The relationship between (ζ) and R_u/H_i, as well as R_d/H_i, for slopes (α) of 45° and 60°, with a water depth (d) of 17.5 cm, and inlet openings (h_s) of (a) 5 cm, (b) 10 cm, and (c) 15 cm

At a water depth (d) of 21 cm shown in Figure 12, the values of R_u/H_i are larger at a slope of 45° compared to 60°. Overall, the values of R_u/H_i tend to be larger at a slope of 45° compared to a slope of 60°. This indicates that the waves climb the breakwater more easily with a gentler slope. The effect of the non-dimensional parameter (ζ) at an open inlet (h_s) of 5 cm (Figure 12-a), at 45° and 60° slope variations (θ), it can be seen that an increase in the value of the non-dimensional parameter (ζ) causes the relative runup trend R_u/H_i to also get larger for a slope of 45°. In contrast, at a slope of 60°, an increase in the value of this parameter causes the trend of the relative runup R_u/H_i to decrease. This suggests that at steeper slopes, increasing this parameter may reduce the ability of waves to climb the breakwater.

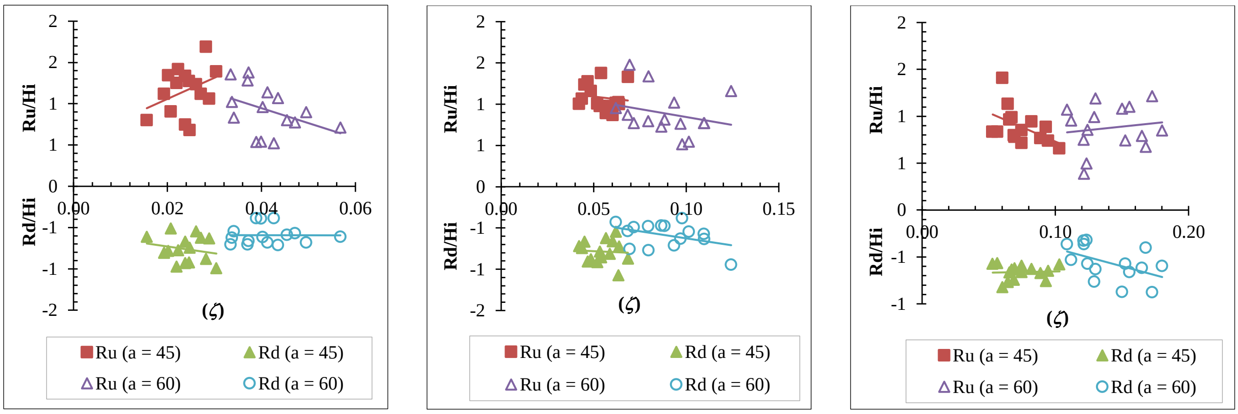

(a) (b) (c)

Figure 12. The relationship between *(ζ)* and R_u/H_i, as well as R_d/H_i, for slopes *(α)* of 45° and 60°, with a water depth (*d*) of 21 cm, and inlet openings (h_s) of (a) 5 cm, (b) 10 cm, and (c) 15 cm

The effect of the non-dimensional parameter *(ζ)* at an inlet opening *(h_s)* of 10 cm (Figure 12-b), at slope variations (θ) of 45° and 60°, shows that as the value of the non-dimensional parameter *(ζ)* increases, the trend of relative runup R_u/H_i tends to decrease. This indicates that at larger inlet openings (10 cm), the effect of this non-dimensional parameter is more dominant in reducing relative runup, independent of slope inclination. The effect of the non-dimensional parameter *(ζ)* on the inlet opening *(h_s)* of 15 cm (Figure 12-c), at 45° and 60° slope variations *(α)*, shows that as the value of the non-dimensional parameter *(ζ)* increases, the relative runup R_u/H_i tends to decrease at 45° slope. In contrast, at a slope of 60°, an increase in the value of this parameter causes the relative runup R_u/H_i to trend upwards. This shows that at the largest inlet opening (15 cm), the effect of this parameter differs depending on the slope. At steeper slopes, increasing this parameter can actually increase the relative runup. To study the effect of *(ζ)* with runup and rundown, simulations of 45° and 60° slope models with closed *(h_{tutup})* and open (h_s = 5c m, 10 cm, and 15 cm) inlets were used at different water depths *(d)* of 24.5 cm.

At a water depth (d) of 24.5 cm shown in Figure 13, the value of R_u/H_i is greater at a slope of 45° than 60°. The value of R_u/H_i tends to be greater at a slope of 45° compared to 60°, indicating that waves climb more easily on breakwaters with slopes that are gentler. The effect of non-dimensional parameters *(ζ)* on R_u/H_i tends to be the same at each slope and inlet opening. At inlet *(h_s)* 5 cm, there is an increasing trend of non-dimensional parameters *(ζ)* as R_u/H_i increases at 45° slope as well as at 60° slope. Inlet *(h_s)* 10 cm shows the same consistency in reducing relative runup, as well as the inlet *(h_s)* 15 cm further clarifies by showing a similar trend. Changing the inlet opening has a consistent effect on R_u/H_i and R_d/H_i, with larger inlet openings generally reducing runup and rundown effects, although this effect can vary based on the slope and the non-dimensional parameters used.

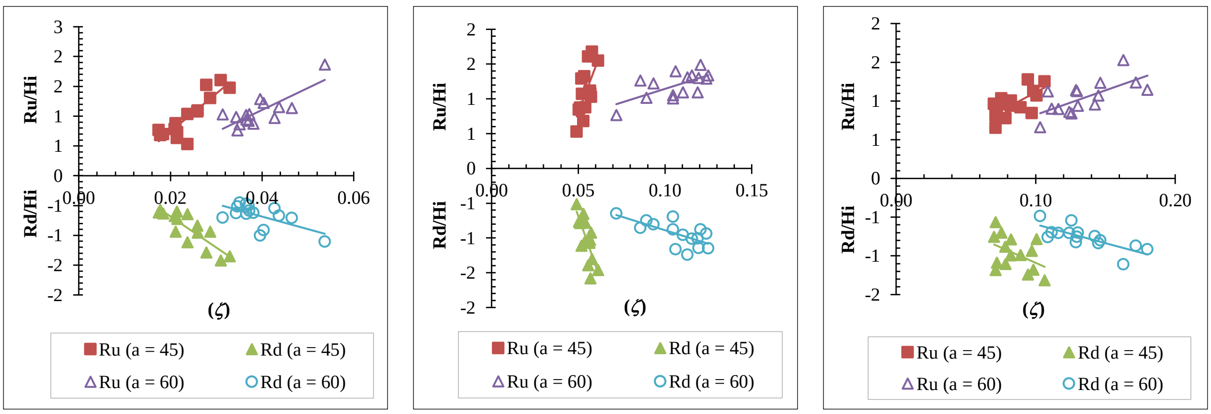

(a) (b) (c)

Figure 13. The relationship between *(ζ)* and R_u/H_i, as well as R_d/H_i, for slopes *(α)* of 45° and 60°, with a water depth (*d*) of 24.5 cm, and inlet openings (h_s) of (a) 5 cm, (b) 10 cm, and (c) 15 cm

4.6. Functional Relationship of Parameter Combination (ψ) to Pressure $\left(\frac{P}{\rho g h_s}\right)$ OWC Breakwater Model

The parameter combination *(ψ)* provides a scaled or ratio measure that describes the interaction between wave height *(H_i)* and water depth *(d)* about wavelength *(L)*. The parameter combination *(ψ)* reflects the effects of resonance and oscillation within the water column. If the incident wave has sufficient energy and an appropriate wavelength, the pressure generated within the column will increase. Figure 14 presents the functional relationship of the parameter combination *(ψ)* to the pressure *(P/ρgh$_s$)* for the slope variation at a water depth *(d)* of 1.75 m and the inlet slope opening *(h$_s$)*. From the graph in Figure 14, it is found that the relationship of the parameter combination *(ψ)* to the pressure *(P/ρgh$_s$)* indicates that as the value of the parameter combination increases, the pressure also increases. This means that there is a positive correlation between the two, indicating that the parameters influence each other significantly in increasing the pressure. For the slope variation, the order of pressure from largest to smallest is 45°, 60°, 90°, 120° and 135°. From this order, it can be concluded that lower slope inclinations (45° and 60°) tend to produce higher pressures compared to larger slope inclinations (120° and 135°). This is due to the changes in pressure distribution due to slope variations that affect fluid flow and dynamics. The order of pressure inlet opening, the graph also shows the order of pressure values by inlet opening from largest to smallest. An inlet opening of *(h$_s$)* 10 cm produces the largest pressure, followed by an inlet opening of *(h$_s$)* 5 cm and the smallest at an inlet opening of *(h$_s$)* 15 cm. This shows that the variation of the inlet opening affects the pressure distribution significantly, where a more optimal opening (in this case 10 cm) gives higher pressure compared to smaller or larger openings.

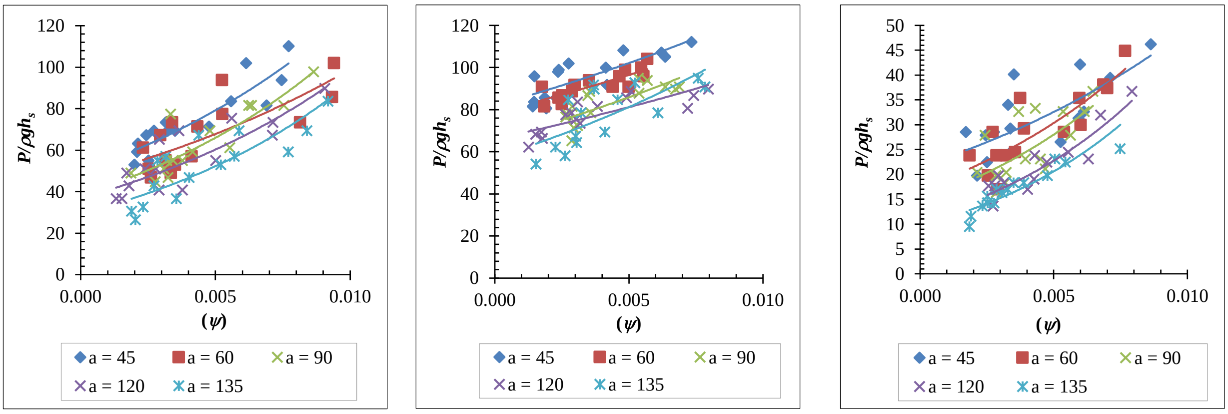

(a) (b) (c)

Figure 14. Graph showing the relationship between (*ψ*) and *P/ρgh* for slope variation *(α)* and a water depth (*d*) of 17.5 cm, with inlet openings (*h$_s$*) of (a) 5 cm, (b) 10 cm, and (c) 15 cm

Figure 15 shows a similar trend, where an increase in the value of the parameter combination *(ψ)* is also followed by an increase in pressure *(P/ρgh$_s$)* at a water depth of 21 cm. This shows the consistent influence of parameter *(ψ)* on pressure at this depth. The variation in the slope of the pressure slope created shows the same trend. This confirms that lower slopes tend to generate higher pressures compared to larger slopes. At a depth of 21 cm, an inlet opening *(h$_s$)* of 10 cm also produces the largest pressure, followed by an inlet opening *(h$_s$)* of 5 cm and the smallest at an inlet opening *(h$_s$)* of 15 cm. This confirms that different inlet openings have a significant effect on pressure distribution, with the optimal opening still being *(h$_s$)* 10 cm.

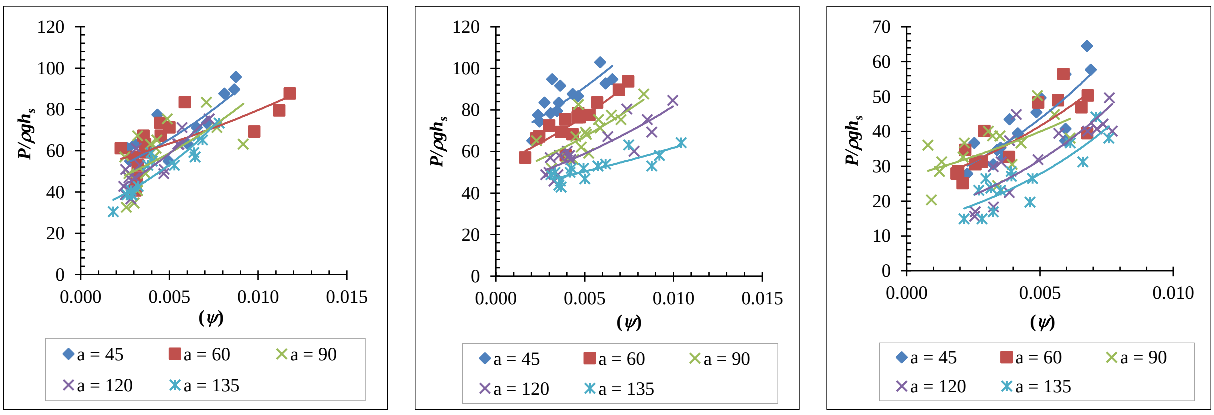

(a) (b) (c)

Figure 15. Graph showing the relationship between (*ψ*) and *P/ρgh* for slope variation *(α)* and a water depth (*d*) of 21 cm, with inlet openings (*h$_s$*) of (a) 5 cm, (b) 10 cm, and (c) 15 cm

Figure 16 also shows an increase in pressure *(P/ρgh$_s$)* as the value of the parameter combination increases *(ψ)*. It is shown that this increasing trend is valid at various depths and slope inclinations. This suggests that a lower slope results in higher pressure. At a water depth (d) of 24.5 cm, an inlet opening *(h$_s$)* of 15 cm produces the largest pressure, followed by an inlet opening *(h$_s$)* of 10 cm and the smallest at an inlet opening *(h$_s$)* of 5 cm. This indicates that at this depth, the 15 cm inlet opening is the most optimal in producing the highest pressure. There is a positive relationship between the value of the parameter combination *(ψ)* and the pressure *($P/\rho gh_s$)* at various depths, indicating the consistent influence of this parameter on pressure. Optimization of the inlet opening at various inlet openings significantly affected the pressure distribution. At depths of 17.5 cm and 21 cm, an inlet opening of *(h_s)* 10 cm is the most optimal, while at a depth of 24.5 cm, an inlet opening of *(h_s)* 15 cm is the most optimal. The results of this study provide important insights into how these parameters can be optimized to improve the efficiency of the hydraulic system through proper pressure regulation. The similarity of the results obtained on the slope variation with those of Bouali & Larbi [15].

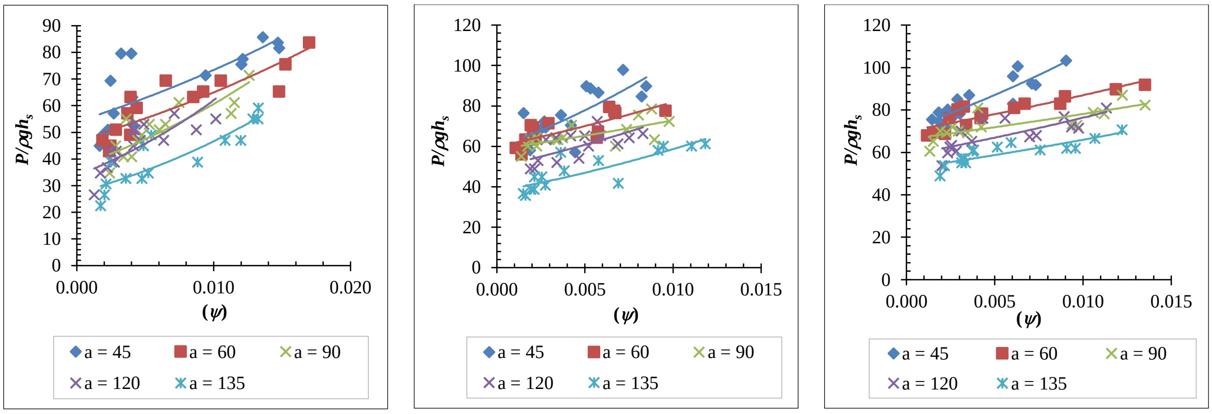

(a) (b) (c)

Figure 16. Graph showing the relationship between (ψ) and $P/\rho gh$ for slope variation *(α)* and a water depth (*d*) of 24.5 cm, with inlet openings (h_s) of (a) 5 cm, (b) 10 cm, and (c) 15 cm

4.7. Physical Implications of Trends Graphic

Energy efficiency is maximized at a 5 cm inlet opening *(h_s)* across all water depths *(d)*, as it effectively captures wave energy and converts it into high internal pressure. This is crucial for designs requiring high wave-breaking efficiency. However, if the inlet is too small, it may restrict airflow, reducing the water column's oscillation response.

A balance between inlet size and effectiveness is achieved at larger openings (10 cm and 15 cm), which allow more water into the column but reduce relative pressure within the system. These designs are suitable for environments with lower wave energy or where extremely high internal pressure is unnecessary.

As the inlet size increases, the relationship between ψ and $P/\rho gh_s$ becomes more linear, indicating that larger openings distribute wave energy more evenly and enhance dissipation. Conversely, a 0.5 cm inlet opening sharply increases relative pressure, making it ideal for breaking high-energy waves efficiently. However, this design may be more sensitive to variations in slope angle.

The influence of the slope angle (slope), with smaller slopes *(α)* of 45° and 60°, tends to be more effective in capturing wave energy for small to medium inlet openings. However, for large inlet openings, gentler slopes (α = 90°, 120°, 135°) can provide more balanced and stable pressure. At small inlet openings (5 cm), smaller slopes (45°-60°) tend to generate higher pressure against *(ψ)*, indicating that designs with smaller slopes will be more effective in breaking waves when the inlet size is limited. However, at steeper angles (120°-135°), the effect of increased pressure remains significant but is more moderate with larger inlet openings.

To maximize the effectiveness of the OWC wave breaker, inlet openings and slope angles must be tailored to specific sea conditions. In high-energy environments with large waves, smaller inlets and steeper slopes optimize energy capture. Conversely, in lower-energy conditions, larger openings and gentler slopes ensure more even energy distribution, generating lower relative pressure while effectively dissipating wave energy.

The design recommendations for large waves and high energy indicate that a small inlet opening (h_s = 5 cm) and steep slopes (α = 45°, 60°) are more efficient options for generating high internal pressure. For small waves and low energy, larger inlet openings (h_s = 10 cm or 15 cm) with gentler slopes (α = 90°, 120°, or 135°) will provide better stability without generating unnecessary excess pressure. The design of wave breakers based on water column oscillation is highly dependent on the interaction between *(ψ)* (wave dimensions relative to wavelength) and $P/\rho gh_s$ (relative pressure), which is influenced by slope and inlet opening. The graphs indicate that variations in slope angles and inlet opening sizes significantly affect the performance of wave breakers. The performance of the OWC wave breaker is shown in Table 5.

Table 5. The performance of the OWC wave breaker

Parameter	(h_s)	(α)	(d)	($P/\rho gh_s$)	Performance
Best model	5 cm	45°- 60°	21 – 24.5 cm	60 – 100	High pressure, stable
Medium model	10 cm	60°- 90°	21 – 24.5 cm	50 – 80	Stable, but not optimal
Less efficient model	15 cm	120°- 135°	24.5 cm	40 – 70	Low pressure, stable

The reason for concluding that the best model is the one with an inlet opening of 5 cm and a slope between 45° and 60° at a water depth of 21 cm to 24.5 cm is based on the analysis of several factors considered in the graphs and research. Although larger inlet openings provide stability in facing large waves, considerations related to energy utilization efficiency and the pressure generated are also key factors.

- The higher relative pressure *($P/\rho g h_s$)* indicates that with an inlet opening of 5 cm, the combination of slope angles of 45° and 60° results in higher pressure in larger inlet openings (10 cm and 15 cm). This higher pressure demonstrates that this model is more efficient in capturing and dissipating wave energy. At the smaller inlet opening (5 cm), the pressure in the oscillation column reaches a sufficiently high and stable value. This is important because higher pressure means more energy can be captured and absorbed by the OWC system, making this design more efficient in reducing wave energy.
- System stability and wave response, however smaller inlet openings tend to lead to sharper pressure increases, and the combination of 45° and 60° slopes helps maintain system stability. The smaller slope helps facilitate the entry of waves into the system more efficiently, resulting in better interaction between the air and water columns. The graph shows that at the 5 cm inlet opening, with this slope, the relative pressure increase *($P/\rho g h_s$)* is consistent, and the exponential trend is more regular compared to the larger inlet opening, where the pressure rise becomes more sloping or unstable.
- The combination of slope *(α)* and inlet opening size *(h_s)* shows a slope of 45° and 60° at a 5 cm inlet opening is an ideal combination of fast response to incoming waves and efficient energy absorption. At larger openings (10 cm and 15 cm), although the stability of the system is better, the pressure rise tends to be slower and less optimal in terms of wave energy absorption. This suggests that, although more stable, the efficiency in capturing wave energy decreases.
- Water depth *(d)* of 21 cm to 24.5 cm shows a model with a fixed 5 cm inlet opening showing good performance in generating relatively high pressures while maintaining system stability. This means that the model can work well at greater water depths, where waves are generally larger and stronger.
- The physical implications and energy efficiency are evident in the 5 cm inlet opening, providing a balance between stability and wave energy absorption efficiency. Although the system may experience higher pressures and less stability compared to larger openings, the combination with slopes of 45° and 60° helps maintain the system's efficiency and stability under various wave conditions. With larger inlet openings (10 cm and 15 cm), the system's stability is better maintained, but the energy absorption efficiency decreases, particularly under larger wave conditions, resulting in a slower pressure response.

4.8. Best Model for Wave Runup and Pressure Formulation of OWC Breakwater Model

The results of the analysis obtained the result that the best model that produces the smallest value of runup *(R_u)* The results of the analysis obtained the result that the best OWC breakwater model that produces on the model slope 60°. The final formulation of the influence of the inlet hole and slope on the magnitude of the runup produced will be based on the OWC breakwater model slope 60°, shown in Figure 17.

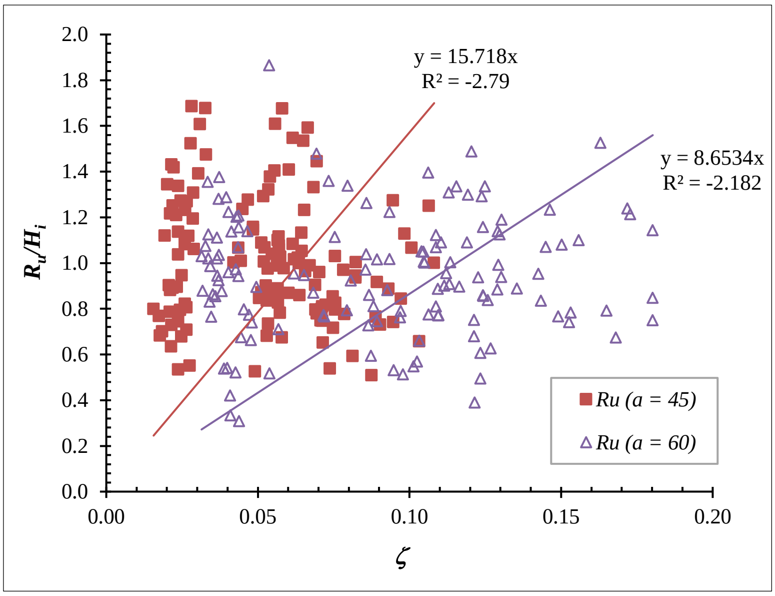

Figure 17. Graph of parameter combination (ζ) with relative runup (R_u/H_i) of OWC breakwater model results 45° and 60°

An empirical equation for the relative runup value *(R_u/H_i)* is obtained as shown in Equation 23:

$$\frac{R_u}{H_i} = a\,.(\zeta) \tag{23}$$

With runup value (R_u)

$$R_u = H_i\,.(a\,.\zeta) \tag{24}$$

where $\zeta = \left(Ir.\frac{h_s.d}{L^2}\right)$ with coefficient values a = 8.6534 for slope 60° dan a = 15.718 for slope 45°, where Ir is the Iribarren number, h_s is the inlet opening, d is the flow depth, and L is the wavelength. Equation 23 applies the value (ζ) ranges from 0.031 to 0.180.

Based on the analysis, it was found that the optimal OWC breakwater model, which generates the highest pressure due to the effect of wave deformation through parameter interaction, is the model with a 45° slope. Therefore, the final formulation of the effect of the inlet hole and slope on the amount of pressure generated will be based on the OWC breakwater model slope 45°.

Parameterized relationship of the interaction between wave height, water depth, wavelength *(ψ)*, and pressure *($P/\rho g h_s$)*. This graph provides an empirical approach to calculate the air pressure *(P)* inside the OWC column as the product of water density *(ρ)*, acceleration of gravity *(g)*, and inlet opening *(h_s)*. The limit of applicability of the graph for the value of *(ψ)* ranges from 0.001 to 0.010. From the data displayed on the graph in Figure 18, the empirical equation for the value of *($P/\rho g h_s$)* is the pressure *(P)* of the OWC breakwater in this study:

$$\frac{P}{\rho g h_s} = 11834\,.(\psi) - 2.6772 \tag{25}$$

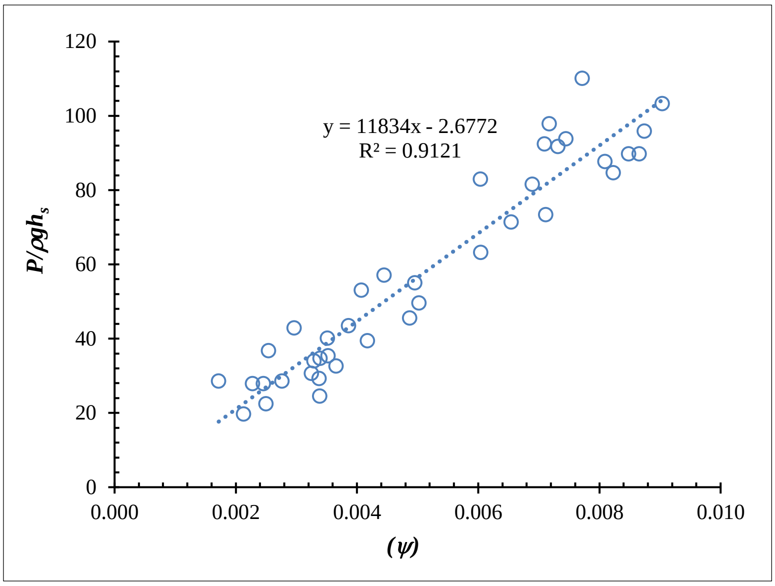

Figure 18. Graph of the combination of parameters (*ψ*) with pressure (*$P/\rho g h_s$*) generated on the OWC breakwater model slope (*θ*) 45°

So that the pressure *(P)* of the OWC breakwater of this study is obtained:

$$P = \rho g h_s\,.(b.\,\psi - c) \tag{26}$$

where $\psi = \left(\frac{H_i.d}{L^2}\right)$ with coefficient values b = 11834 and c = 2.6772, where ρ is the density of water, g is the acceleration of gravity, h_s is the inlet opening, H_i is the wave height, d is the depth of flow, and L is the wavelength. The novel result of this research is the empirical equation of runup pressure *(R_u)* and *(P)* on the OWC breakwater model against the combination parameter. The use of cavities in breakwater structures has the advantage of saving material and being environmentally friendly this breakwater functions as a breakwater and also as a wave energy converter.

The non-dimensional parameter ψ indicates the effect of wave height and water depth relative to wavelength, which affects energy transfer efficiency. The non-dimensional parameter ζ describes the proportion of wave height to wavelength, providing information about wave intensity relative to wave runup on the OWC breakwater. This trend is illustrated in Figures 17 and 18, which connect the non-dimensional parameters with OWC performance, and this observation is relevant for the design of OWC at specific locations and its impact on engineering decision-making.

Several studies examine the integration of breakwaters with Oscillating Water Column (OWC) technology and their benefits. Falcão et al. [25] provides a comprehensive review of the lifetime of the Pico OWC power plant, offering insights into its operation and shutdown. Gaspar et al. [26] presents findings on the impact of chamber wall slope on the energy conversion efficiency of onshore OWCs. He et al. [27] examines the hydrodynamic efficiency of pile-supported breakwaters combined with OWC systems. Lee et al. [28] highlights key parameters that influence the performance of caisson-based OWC energy systems. Liu et al. [29] offers experimental data on the performance of OWC chambers under irregular wave conditions. Zheng et al. [30] proposes a theoretical model for integrating OWC systems into coastal structures and breakwaters. Thaha et al. [31] suggests that breakwaters can evolve from wave energy breakers to wave energy collectors without sacrificing their primary role in coastal protection. The incorporation of Wave Energy Converters (WEC) into coastal structures is generally more straightforward for new constructions than for existing ones.

Analyzing the impact of the spacing parameter (S) of the OWC device on a conventional breakwater reveals that the vertical wall tends to concentrate more wave energy within the space of the integrated oscillating wave (OWC) device, thus improving its efficiency. This effect intensifies as the spacing (S) increases. The analysis of both partial and full converging breakwaters concludes that this novel geometry, which channels a portion of incoming wave energy into the OWC chamber, significantly enhances the efficiency of the OWC device array within a specific range of wave periods [32]. Venkateswarlu et al. [33] observed improved efficiency of Oscillating Water Column (OWC) devices at higher frequencies, with increases in the height, width, and chamber length dimensions of bottom-standing breakwaters (BSBs). The research suggests using a pair of BSBs with a chamber length equal to the water depth to achieve optimal efficiency [34]. A deep understanding of the fundamental principles and challenges related to this innovative technology is crucial. In the wave energy sector, Oscillating Water Column (OWC) systems, which are available in both fixed and floating configurations, represent a key category. OWC devices play a significant role in the proportion of prototype wave energy converters currently deployed in offshore waters.

Wang et al. [35] demonstrates that optimizing power extraction can be achieved by using larger transverse spacing, which increases the capture width ratio across a broader range of wave frequencies. This results in a 55.8% improvement between larger and smaller transverse spacing conditions. Furthermore, a moderate slope profile was identified as the most effective choice for enhancing performance when larger transverse spacing is applied. Tsai et al. [36] found that under irregular wave conditions, the maximum pressure generated was approximately 50% higher than under regular wave conditions. The experiments showed that the combination of M-OWC and C-OWC significantly contributes to reducing wave pressure on the caisson breakwater structure during storm events. This highlights the dual advantages of using OWC devices in front of breakwaters, as they both absorb wave energy and reduce the force applied to the breakwater. Zhang et al. [37] The maximum and minimum hydrodynamic efficiencies occur when the system is positioned at the wave nodes and antinodes within the standing wave field. Proper design and area adjustments can reduce wave reflection and increase wave power extraction.

Development of the OWC breakwater model as a wave energy dissipator or converter examines dimensionless parameters, such as the inlet opening size (h_s) and the slope angle (α), which can be adjusted based on environmental conditions. However, the implementation of the model or prototype has certain limitations. Laboratory experiments using three variations of the inlet opening (h_s) have not analyzed the pressure loss due to the inlet opening passing through the incident wave height (H_i) nor the stability of the structure due to limited laboratory testing time. The OWC model breakwater still requires three-dimensional testing to obtain more realistic results, ensuring the structural strength to withstand maximum pressure and avoid damage when operating in extreme sea wave conditions. The advantages of the OWC breakwater model include its dual functionality as a breakwater or an energy catcher with OWC technology. The results of the relative runup analysis indicate that the OWC breakwater with a slope angle of 60° performs better as a wave barrier structure. Meanwhile, a slope angle of 45° is more optimal for capturing wave energy when used as an energy catcher. The use of the OWC breakwater also offers economic advantages and efficiency in the use of construction materials compared to other types of wave breakers, such as the rubble mound type.

Table 6 presents a detailed comparison between this research and relevant studies on inlet opening geometry and slope angles in Oscillating Water Column (OWC) system design. The comparison highlights key aspects, including inlet openings, slope variations, and research differences.

Table 6. Comparison with relevant previous research

Researchers	Main focus	Difference
Iturrioz et al. [8]	Inlet opening: • This study explored small aperture sizes (2 mm to 50 mm) using Open FOAM simulations. • It does not focus on tilt but rather on the effect of wave height and slot size on performance.	• The study focused on the larger inlet opening sizes (5 cm, 10 cm, and 15 cm) and slope as the main parameters. • The Iturrioz et al. study was more of a numerical simulation, while the study was experimental, focusing more on relative pressure and slope effects.
Raj et al. [9]	Inlet opening: • Although this study did not directly examine the geometry of the inlet opening, it introduced a port wall to improve the hydrodynamic efficiency of OWC. Slope angle: • There is no focus on the variation of slope angles, with emphasis on resonance length and harbor walls.	• This study directly tested the variation of inlet slope and opening against pressure efficiency, While Raj et al.'s study focused on improving performance with environmental modifications such as the addition of port walls.
Elhanafi et al. [10]	Inlet opening: • This research examines the effects of depth and thickness of the underwater lip on the performance of OWC. Slope angle: • There is no focus on the inclination angle or inlet opening at the surface, concentrating on the underwater geometric design.	• This study places greater emphasis on the interaction between the surface inlet opening geometry and the inclination concerning pressure and efficiency. The study by Elhanafi et al. focuses more on underwater geometric modifications for hydrodynamic performance.
Ning et al. [11]	Inlet opening: • Focus on U-shaped geometry with modifications to the height of the vertical channel and the width of the space, without explicit focus on the inlet opening. Slope angle: • No specific study on the slope in this research.	• This study examines how variations in the inlet opening and slope impact pressure and performance, while Ning et al. focus on general geometric modifications of the space and vertical channel.
Vyzikas et al. [12]	Inlet opening: • This research examines four different OWC geometries, focusing on variations in spatial geometry. • There is no direct focus on variations in inlet openings as in this study. Slope angle: • There is no focus on variations in inclination angles in this research.	• This study focuses on inlet openings and inclination as key variables to enhance pressure efficiency, whereas the research by Vyzikas et al. is more about testing various overall geometries.
Deng et al. [13]	Inlet opening: • Focus on the opening ratio at the top of the chamber with a horizontal bottom plate. Slope angle: • There is no focus on the slope in this study.	• This study investigates how variations in slope and inlet opening affect pressure. Deng et al. focus more on the effects of the geometry of the horizontal bottom plate on wave absorption efficiency.
Mahnamfar & Altunkaynak [14]	Inlet opening: • The study focuses on the optimization of the geometry of the OWC space in general, without specific emphasis on variations of the inlet opening. Slope angle: • It does not test the angle of inclination but rather the optimization of the design space.	• This study explores how variations in the geometry of the inlet opening and inclination affect pressure, while Mahnamfar and Altunkaynak focus on the overall geometry optimization to enhance energy extraction.
Bouali & Larbi [15]	Inlet opening: • Utilizing various geometric configurations, in general, to enhance energy conversion performance without focusing on specific inlet openings. Slope angle: • There is no specific focus on the variation of the angle of inclination in this study.	• This study focuses on specific parameters such as inlet openings and inclination, whereas Bouali and Larbi investigate geometric optimization in general without a detailed investigation of inlet parameters.
Oh & Han [16]	Inlet opening: • This research focuses on the effects of inlet geometry on wave energy capture efficiency. Slope angle: • There is no explicit focus on inclination.	• This study involves a detailed examination of how the inlet opening and inclination affect relative pressure. In contrast, Oh and Han only focus on the inlet opening in the context of energy capture efficiency.

Table 7 illustrates a comparison that explains the advantages and limitations of the OWC physical model. Aspects of comparing are the simplicity of the experiment, reproducibility, hydrodynamic modeling, real-world representation, the dimension being tested (2D), dimensionless parameters, measurement of pressure, implementation facilities, and structural stability analysis.

Table 7. Comparison of the advantages and limitations of the physical OWC model

Aspects	Advantages	Limitations
The simplicity of the experiment	Physical modeling provides direct and measurable results.	It cannot fully capture 3D interactions (lateral effects).
Reproducibility	Clear experimental procedures can be repeated under similar conditions.	Depending on the accuracy of measurements and control of variables in the flume.
Hydrodynamic modeling	Capturing real hydrodynamic phenomena, such as wave reflection, runup, and air pressure.	Does not include scale effects that are difficult to represent, such as micro turbulence.
Real-world representation	The 1:20 scale allows observation of wave patterns relevant to coastal conditions.	It covers only specific conditions; Parameters such as wind and multi-dimensional effects are ignored.
The dimension being tested (2D)	This study provides an initial analysis of the efficiency and pressure distribution in an Oscillating Water Column (OWC) under two-dimensional conditions.	This research does not take into account three-dimensional effects, such as lateral energy dispersion or lateral stability.
Dimensionless parameters	Parameters such as ψ and ζ assist in generalizing results to various wave conditions.	Generalizing results to complex conditions requires additional testing or numerical simulations.
Measurement of pressure	Air pressure and runup can be measured directly, yielding concrete data.	This measurement is sensitive to device errors, especially in turbulent wave conditions.
The implementation facilities	Flume and physical models are easy to construct and operate in the laboratory.	A sufficiently large laboratory space and resources are required to replicate.
Structural stability analysis	Provides a basis for the design of more efficient structural geometry.	Structural stability has not been tested; material testing and numerical simulations are required.

Integrating OWCs with breakwaters allows for more efficient space utilization in coastal areas, reducing the need for separate installations. Combining these two functions in one structure can reduce construction and maintenance costs compared to building the protective structure and energy system separately. This approach offers an eco-friendly renewable energy source, contributing to a reduction in reliance on fossil fuels while preserving the breakwater's primary function of protecting the coast from erosion and wave damage. The challenges associated with OWC integration involve the requirement for complex designs and materials capable of withstanding harsh oceanic conditions. Although economically viable in the long term, the initial investment for this integration is high. OWC systems integrated with breakwaters require regular maintenance to ensure reliability and optimal performance. Integrating OWCs with breakwaters provides a dual solution for renewable energy generation and coastal protection. This study shows the promise of this approach, though challenges persist for large-scale implementation. Technological advancements and an improved understanding of wave interactions with integrated structures could enhance its future role in energy management and coastal protection. While this research lays the groundwork for OWC development, further validation through 3D testing or numerical simulations is necessary.

4.9. Development of OWC Breakwater Model for Field Use

A case example using the empirical equations that have been obtained, an island with approximately 15 households requires 520.86 (MW) of electrical power to serve all families on the island, requiring a pressure of 17,400,000 N/m^2 (Pascal) or 17.40 (MPa) on the OWC breakwater to achieve this power. Water density *(ρ)* 1026 kg/m^3, acceleration of gravity *(g)* 9.81 m/s^2, wave height *(H_i)* 1.5 m, flow depth *(d)* 5 m, wavelength *(L)* 10 m. The inlet opening *(h_s)* required to generate the requisite pressure.

Using Equation 26, the steps are as follows:

- Substitute the known values into the equation:

$$17{,}400{,}000 \ = 1026\,.\,9.81\,.\,h_s\,.\left(11834\,.\frac{1.5\,.\,5}{10^2} - 2.6772\right)$$

- Simplify the inside of the brackets first:

$$11834\left(\frac{1.5\,.\,5}{10^2}\right) = 11834\left(\frac{1.5\,.\,5}{100}\right) = 887.55$$

$$887.55 - 2.6772 = 884.8728$$

- Substitute the result into Eq.:

$$17{,}400{,}000 \ = 1026\,.\,9.81\,.\,h_s\,.\,884.8728$$

- Simplify the equation:

$$17{,}400{,}000 \ = 1026\,.\,9{,}81.\,884.8728\,.\,h_s$$

$$17{,}400{,}000 \ = 8{,}906{,}297.82.\,h_s$$

- Calculate the height of the inlet opening h_s:

$$h_s = \frac{17{,}400{,}000}{8{,}906{,}297.82} \quad \Rightarrow \quad h_s \approx 1.954\,m$$

The height of the inlet opening (h_s) required to obtain a pressure of 17,400,000 N/m^2 is about 1.954 m or 2.00 m. This indicates that the inlet opening requisite to achieve this pressure under wave conditions and flow depths is at the environmental conditions of the island.

5. Conclusion

This study has demonstrated the critical role of wave deformation in OWC breakwater models, which results from the interaction between wave parameters, model geometry, and depth. The findings highlight a positive correlation between the non-dimensional parameter (ψ) and relative pressure $(P/\rho g h_s)$ at varying depths, showcasing the consistent influence of these parameters on pressure distribution. A shallower slope increased pressure while optimizing the inlet opening size considerably affected pressure distribution. For example, at depths of 17.5 cm and 21 cm, inlet openings (h_s) of 5 cm and 10 cm were most effective, whereas, at 24.5 cm, an inlet opening of 15 cm performed best. The optimal configuration for the breakwater was an inlet opening of 5 cm, with a slope between 45° and 60°, and water depths ranging from 21 cm to 24.5 cm. This configuration yielded higher relative pressure $(P/\rho g h_s)$ and system stability, signifying improvement in wave energy utilization.

The study also revealed that non-dimensional parameters (ζ) influenced the relative wave runup (R_u/H_i) similarly across slopes and inlet sizes. For instance, a 5 cm inlet opening showed an increasing trend in ζ as Ru/Hi increased at slopes of 45° and 60°, while inlet sizes of 10 cm and 15 cm consistently reduced relative runup. These results confirm the importance of tuning inlet size and slope to manage the wave runup (R_u/H_i) and rundown (R_d/H_i) well. Larger inlet openings generally reduced these effects, but the impact varied with slope and parameter configuration.

Empirical equations derived from experimental testing estimate wave runup and pressure, offering the use of tools for OWC breakwater design. The wave runup equation is:

$R_u = H_i\,.\,(a\,.\,\zeta)$, where $\zeta = \left(Ir.\frac{h_s.\,d}{L^2}\right)$, and a = 8.6534 for a 60° slope, a = 15.718 for a 45 ° slope.

The pressure equation is:

$P = \rho g h_s\,.\,(b\,.\,\psi - c)$, where $\psi = \left(\frac{H_i.\,d}{L^2}\right)$, b = 11834 and c = 2.6772.

These equations enable the practical application of laboratory findings to estimate wave runup and pressure in OWC breakwater design.

This research advances knowledge by demonstrating how slope angle, inlet opening size, and depth influence pressure and wave behavior. It provides a scientific basis for optimizing OWC breakwater configurations to maximize efficiency and structural stability. Compared to traditional breakwaters, OWC designs are cost-effective, offering dual functionality as both a wave attenuator and an energy-harnessing structure. However, this study is limited to three inlet size variations and does not include pressure loss analysis through the inlet. Structural stability under operational ocean conditions was also not examined, and 3D testing is needed to simulate realistic wave scenarios. Future research addressing these aspects will improve the applicability and reliability of OWC breakwater designs. The study concludes that OWC breakwaters are highly promising for coastal applications, with specific configurations tailored to balance wave energy utilization and system durability. This makes them a sustainable and efficient alternative to traditional rubble mound breakwaters.

6. Declarations

6.1. Author Contributions

Conceptualization, S, R.T.L., R.K., and C.P.; methodology, S., R.K., and C.P.; software, S.; validation, S., R.T.H., R.K., and C.P.; formal analysis, S.; investigation, S.; resources, S.; data curation, S.; writing—original draft preparation, S.; writing—review and editing, S., R.T.L., R.K., and C.P.; visualization, S.; supervision, R.T.L., R.K., and C.P.; project administration, S.; funding acquisition, S. All authors have read and agreed to the published version of the manuscript.

6.2. Data Availability Statement

The data presented in this study are available on request from the corresponding author.

6.3. Funding

The authors received no financial support for the research, authorship, and/or publication of this article.

6.4. Conflicts of Interest

The authors declare no conflict of interest.

7. References

[1] Heath, T. V. (2012). A review of oscillating water columns. Philosophical Transactions of the Royal Society A: Mathematical, Physical and Engineering Sciences, 370(1959), 235–245. doi:10.1098/rsta.2011.0164.

[2] Suh, K. D., Park, J. K., & Park, W. S. (2006). Wave reflection from partially perforated-wall caisson breakwater. Ocean Engineering, 33(2), 264–280. doi:10.1016/j.oceaneng.2004.11.015.

[3] Rageh, O. S., & Koraim, A. S. (2010). Hydraulic performance of vertical walls with horizontal slots used as breakwater. Coastal Engineering, 57(8), 745–756. doi:10.1016/j.coastaleng.2010.03.005.

[4] Yuwono, N., & Sriyana, I. (2022). Wave Transmission and Energy Dissipation in a Box Culvert-Type Slotted Breakwater. Advances in Technology Innovation, 7(4), 270.

[5] Koraim, A. S. (2014). Hydraulic characteristics of pile-supported L-shaped bars used as a screen breakwater. Ocean Engineering, 83, 36–51. doi:10.1016/j.oceaneng.2014.03.016.

[6] Lopa, R. T., & Rohani, I. (2018). Breakwater Analysis in Bamballoka, Pasangkayu Regency. Bandar: Journal of Civil Engineering, 1(1), 25-29. (In Indonesian).

[7] Bungin, E. R., Pallu, S., Thaha, M. A., & Lopa, R. T. (2020). The effect of asymmetric submerged structure series on wave deformation. 9 February, 2017, Pekanbaru, Indonesia. (In Indonesian).

[8] Iturrioz, A., Guanche, R., Lara, J. L., Vidal, C., & Losada, I. J. (2015). Validation of OpenFOAM® for Oscillating Water Column three-dimensional modeling. Ocean Engineering, 107, 222–236. doi:10.1016/j.oceaneng.2015.07.051.

[9] Daniel Raj, D., Sundar, V., & Sannasiraj, S. A. (2019). Enhancement of hydrodynamic performance of an Oscillating Water Column with harbour walls. Renewable Energy, 132, 142–156. doi:10.1016/j.renene.2018.07.089.

[10] Elhanafi, A., Fleming, A., Macfarlane, G., & Leong, Z. (2017). Underwater geometrical impact on the hydrodynamic performance of an offshore oscillating water column–wave energy converter. Renewable Energy, 105, 209–231. doi:10.1016/j.renene.2016.12.039.

[11] Ning, D. zhi, Guo, B. ming, Wang, R. quan, Vyzikas, T., & Greaves, D. (2020). Geometrical investigation of a U-shaped oscillating water column wave energy device. Applied Ocean Research, 97(September), 102105. doi:10.1016/j.apor.2020.102105.

[12] Vyzikas, T., Deshoulières, S., Barton, M., Giroux, O., Greaves, D., & Simmonds, D. (2017). Experimental investigation of different geometries of fixed oscillating water column devices. Renewable Energy, 104, 248–258. doi:10.1016/j.renene.2016.11.061.

[13] Deng, Z., Wang, C., Wang, P., Higuera, P., & Wang, R. (2019). Hydrodynamic performance of an offshore-stationary OWC device with a horizontal bottom plate: Experimental and numerical study. Energy, 187, 115941. doi:10.1016/j.energy.2019.115941.

[14] Mahnamfar, F., & Altunkaynak, A. (2017). Comparison of numerical and experimental analyses for optimizing the geometry of OWC systems. Ocean Engineering, 130, 10–24. doi:10.1016/j.oceaneng.2016.11.054.

[15] Bouali, B., & Larbi, S. (2013). Contribution to the geometry optimization of an oscillating water column wave energy converter. Energy Procedia, 36, 565–573. doi:10.1016/j.egypro.2013.07.065.

[16] Oh, J. S., & Han, S. H. (2012). Inlet geometry effect of wave energy conversion system. Journal of Mechanical Science and Technology, 26(9), 2793–2798. doi:10.1007/s12206-012-0726-7.

[17] Triatmodjo, B. (1999). Coastal Engineering. Beta Offset, Yogyakarta, Indonesia. (In Indonesian).

[18] McCormick, M. E. (2013). Ocean wave energy conversion. Courier Corporation, Massachusetts, United States.

[19] Hughes, S. A. (1993). Physical models and laboratory techniques in coastal engineering. World Scientific Publishing Company, Singapore.

[20] Huddiankuwera, A., Rachman, T., Thaha, M. A., & Dewa, S. (2022). Wave Deformation on Sloping Hollow Breakwater. International Journal of Engineering Trends and Technology, 70(10), 188–194. doi:10.14445/22315381/IJETT-V70I10P218.

[21] Koraim, A. S., Heikal, E. M., & Abo Zaid, A. A. (2014). Hydrodynamic characteristics of porous seawall protected by submerged breakwater. Applied Ocean Research, 46, 1–14. doi:10.1016/j.apor.2014.01.003.

[22] Dean, R. G., & Dalrymple, R. A. (1984). Water wave mechanics for engineers and scientists. World Scientific Publishing Company, Singapore. doi:10.1029/eo066i024p00490-06.

[23] Soewarno, S. (1995). Hydrology: Application of Statistical Methods for Data Analysis. Nova, Bandung, Indonesia. (In Indonesian).

[24] Goel, A. (2011). ANN-Based Approach for Predicting Rating Curve of an Indian River. ISRN Civil Engineering, 2011, 1–4. doi:10.5402/2011/291370.

[25] Falcão, A. F. O., Sarmento, A. J. N. A., Gato, L. M. C., & Brito-Melo, A. (2020). The Pico OWC wave power plant: Its lifetime from conception to closure 1986–2018. Applied Ocean Research, 98, 102–104. doi:10.1016/j.apor.2020.102104.

[26] Gaspar, L. A., Teixeira, P. R. F., & Didier, E. (2020). Numerical analysis of the performance of two onshore oscillating water column wave energy converters at different chamber wall slopes. Ocean Engineering, 201, 107–119. doi:10.1016/j.oceaneng.2020.107119.

[27] He, F., Zhang, H., Zhao, J., Zheng, S., & Iglesias, G. (2019). Hydrodynamic performance of a pile-supported OWC breakwater: An analytical study. Applied Ocean Research, 88, 326–340. doi:10.1016/j.apor.2019.03.022.

[28] Lee, H. H., Chiu, Y.-F., Lin, C.-Y., Chen, C.-H., & Huang, M.-H. (2016). Parametric Study on a Caisson Based OWC Wave Energy Converting System. World Journal of Engineering and Technology, 04(03), 213–219. doi:10.4236/wjet.2016.43d026.

[29] Liu, Z., Xu, C., Shi, H., & Qu, N. (2020). Wave-flume tests of a model-scaled OWC chamber-turbine system under irregular wave conditions. Applied Ocean Research, 99, 102–141. doi:10.1016/j.apor.2020.102141.

[30] Zheng, S., Zhang, Y., & Iglesias, G. (2019). Coast/breakwater-integrated OWC: A theoretical model. Marine Structures, 66, 121–135. doi:10.1016/j.marstruc.2019.04.001.

[31] Thaha, A., Maricar, F., Aboe, A. F., & Dwipuspita, A. I. (2015). The breakwater, from wave breaker to wave catcher. Procedia Engineering, 116(1), 691–698. doi:10.1016/j.proeng.2015.08.352.

[32] Didier, E., & Teixeira, P. R. F. (2024). Numerical analysis of 3D hydrodynamics and performance of an array of oscillating water column wave energy converters integrated into a vertical breakwater. Renewable Energy, 225, 120–297. doi:10.1016/j.renene.2024.120297.

[33] Venkateswarlu, V., Panduranga, K., Vijay, K. G., & Behera, H. (2024). Evaluation of oscillating water column efficiency in the presence of multiple bottom-standing breakwaters under oblique waves. Physics of Fluids, 36(11), 117–175. doi:10.1063/5.0237370.

[34] Gayathri, R., Chang, J. Y., Tsai, C. C., & Hsu, T. W. (2024). Wave Energy Conversion through Oscillating Water Columns: A Review. Journal of Marine Science and Engineering, 12(2), 1–22. doi:10.3390/jmse12020342.

[35] Wang, C., Zhang, Y., Xu, H., & Chen, W. (2024). Wave power extraction from an integrated system composed of a three-unit oscillating water column array and an inclined breakwater. Renewable and Sustainable Energy Reviews, 202, 114–645. doi:10.1016/j.rser.2024.114645.

[36] Tsai, C. P., Fan, C. Y., Chen, Y. C., & Ko, C. H. (2024). Experimental Study of wave pressure on breakwater-integrated OWC Wave Energy Converter. In ISOPE International Ocean and Polar Engineering Conference (ISOPE), 16-21 June, 2024, Rhodes, Greece.

[37] Zhang, Y., Zhu, W., Xu, Q., Kong, D., & Dong, X. (2024). Hydrodynamic performance of a pile-supported oscillating water column breakwater in front of a partially reflecting seawall. Physics of Fluids, 36(7), 077–139. doi:10.1063/5.0219892.